

# Low energy meson spectrum from a QCD approach based on many-body methods

D. A. Amor-Quiroz,<sup>1,\*</sup> T. Yépez-Martínez,<sup>2,†</sup> P. O. Hess,<sup>1,‡</sup> O. Civitarese,<sup>2,§</sup> and A. Weber<sup>3,¶</sup>

<sup>1</sup> *Instituto de Ciencias Nucleares, Universidad Nacional Autónoma de México Circuito Exterior, C.U., Apartado postal 70-543, 04510 México D.F., México.*

<sup>2</sup> *Departamento de Física, Universidad Nacional de La Plata, C.C. 67 (1900), La Plata, Argentina.*

<sup>3</sup> *Instituto de Física y Matemáticas, Universidad Michoacana de San Nicolás de Hidalgo, Edificio C-3, Ciudad Universitaria, Apartado Postal 2-82, 58040 Morelia, Michoacán, México*

(Dated: October 5, 2018)

The TDA and RPA many-body methods are applied to a QCD motivated Hamiltonian in the Coulomb gauge. The gluon effects in the low energy domain are accounted for by the Instantaneous color-Coulomb Interaction between color-charge densities, approximated by the sum of a Coulomb ( $\alpha/r$ ) and a confining linear ( $\beta r$ ) potentials. We use the eigenfunctions of the harmonic oscillator as a basis for the quantization of the quark fields, and discuss how suitable this basis is in various steps of the calculation. We show that the TDA results already reproduce the gross-structure of the light flavored meson states. The pion-like state in the RPA description, which is a highly collective state, is in a better agreement with the experimental value. The results are related to other non-perturbative treatments and compared to experimental data. We discuss the advantages of the present approach.

PACS numbers: 12.38.-t, 12.40.Yx, 14.40.-n, 21.60.Fw

Keywords: Low energy meson spectrum, non-perturbative QCD, TDA and RPA results.

## I. INTRODUCTION

*Quantum Chromodynamics* (QCD) is the theory of the strong interactions. It has been verified in numerous experiments and is well understood at high energies where, due to asymptotic freedom, the coupling constant is small and perturbative techniques work well. At low energy, however, QCD is a highly non-perturbative theory.

Up to now, only *Lattice Gauge Theory* (LGT) has been able to obtain reliable results from first principles (see, *e.g.*, [1] for a recent overview). There are also disadvantages to LGT, principally the huge numerical effort involved, but also the difficulties to simulate light quarks with realistic current masses, to identify the states for a given spin (due to the breaking of rotational symmetry in the formulation of LGT), to obtain excited states, etc. In recent years, some improvements in the implementation of LGT have been achieved in describing low lying hadron states [2, 3] and highly excited meson states [4]. The Dyson-Schwinger equation (DS) method applied to low energy QCD has several advantages, particularly describing in a self-consistent way the dynamical generation of the constituent quark masses and implementing the axial-vector Ward-Takahashi identity exactly [5]. However, the DS method has its own drawbacks, mainly the absence of clear prescriptions to truncate diagrammatic contributions.

The implementation of schematic models in QCD-motivated Hamiltonians has provided the complete spectrum of glueball states [6] and hadrons [7, 8]. In all these attempts, it was shown that the use of methods based on group theory and diagonalization in small spaces can yield analytic results in certain limits. The numerical efforts are less demanding compared to LGT, the rotational symmetry is maintained, and the identification of the complete spectrum is feasible.

The formulation of QCD in the Coulomb gauge [9, 10] has been widely used. Several systems described by the non-perturbative regime of QCD have been examined in this framework. The glueball spectrum, studied by LGT [11, 12], was well reproduced in [13, 14]. The calculations for systems involving heavy quarks [15], like charmonium and bottomonium, have approximately reproduced the available data. The charmonium hybrid meson spectrum and their radiative transitions, including controversial exotic states, were calculated in [15, 16] and compared to LGT results [17, 18]. Finite temperature studies focused on the Yang-Mills sector of the theory [19, 20] have been able

---

\*Electronic address: arturo.amor@nucleares.unam.mx

†Electronic address: yepez@fisica.unlp.edu.ar

‡Electronic address: hess@nucleares.unam.mx

§Electronic address: osvaldo.civitarese@fisica.unlp.edu.ar

¶Electronic address: axel@ifm.umich.mx

to describe the possibility of a phase transition for this system, as well as its thermal properties described before by LGT [21, 22].

As a starting point for a different approach to diagonalizing the QCD Hamiltonian that employs the effective formulation developed in [23], analytic results were obtained in [24] for light quark systems restricted to one orbital level. This approach was extended to an arbitrary number of orbital levels by applying a diagonalization to the kinetic energy of the pure quark sector of the QCD Hamiltonian in a finite volume [25]. It was shown that the use of the harmonic oscillator basis has several practical advantages as it leads to analytical expressions for the relevant matrix elements. In this basis it is also straightforward to subtract the contributions of the center of mass motion. Though the harmonic oscillator states represent a non-relativistic basis, which implies that one has to use many states to approximate relativistic states, its use is advantageous. Recently, we have investigated the implementation of many-body methods in a  $SO(4)$ -model for quarks [26, 27], which leads to a pion-like state with high collectivity.

In this contribution we go further and try to extract information about the microscopic structure of low energy meson states, by approximating the QCD Instantaneous color-Coulomb Interaction (QCD-IcCI) which has been derived in [9, 10]. In [23, 28], the momentum dependence of the QCD-IcCI has been studied for a static quark-antiquark pair, using a self-consistent mean field approximation. It was shown that in coordinate space it corresponds to a linear potential, of the type found in LGT. Motivated by these results, we substitute the QCD-IcCI by a Coulomb plus linear potential, the latter being the confining part of the quark-quark interaction. This potential acts instantaneously and its use may be questioned for light quarks. In any case, the effective potential can only be considered as a first approximation, and the effects of dynamical gluons should eventually be included [23]. The main objective of the present work is to show that there is a possibility to improve and significantly simplify the burden of calculations in low-energy non-perturbative QCD by using many-body methods, and that the harmonic oscillator basis is well suited for this task. The strategy will be explained in detail in the course of the paper.

The paper is organized as follows: in Section II, the effective QCD Hamiltonian derived in [23] will be discussed and the approximations will be justified. The Hamiltonian is then rewritten in terms of the harmonic oscillator basis and its operators. A prediagonalization is applied to the kinetic plus mass terms, after which it is possible to define effective quark and antiquark operators. In Section III, the Tamm-Dancoff-Approximation (TDA) and the Random-Phase-Approximation (RPA) are applied to the Hamiltonian, and the spectrum of meson states viewed as collective states is calculated. We will show that the meson spectrum is, to a large extent, reproduced. While the energy of the pion-like state in TDA is higher than the experimental data, the RPA result for the same state is in better agreement with the experimental value. We also compare our results to the spectrum obtained in [29], where a continuum basis for the description of the meson states was used and the same approximations were applied. Since the RPA method introduces pair correlations in the ground state, the interactions that account for them are identified and their effects quantified. In subsection III B, the renormalization of the quark masses and couplings is described. We present our conclusions in Section IV. The technical details of the approach are relegated to five appendices.

## II. THE QCD HAMILTONIAN AT LOW ENERGY

As we have already mentioned in Section I, QCD has been widely studied in its canonical Coulomb gauge representation. In Ref. [23], it was shown how confinement and the constituent particles (quarks and gluons) can be treated simultaneously within this gauge. The QCD Hamiltonian in the canonical Coulomb gauge representation is given by [9, 10]

$$\begin{aligned} \mathbf{H}^{QCD} = & \int \left\{ \frac{1}{2} [\mathcal{J}^{-1} \mathbf{\Pi}^{tr} \cdot \mathcal{J} \mathbf{\Pi}^{tr} + \mathcal{B} \cdot \mathcal{B}] - \bar{\psi} (-i\boldsymbol{\gamma} \cdot \nabla + m) \psi - g \bar{\psi} \boldsymbol{\gamma} \cdot \mathbf{A} \psi \right\} d\mathbf{x} \\ & + \frac{1}{2} g^2 \int \mathcal{J}^{-1} \rho^c(\mathbf{x}) \langle c, \mathbf{x} | \frac{1}{\nabla \cdot \mathcal{D}} (-\nabla^2) \frac{1}{\nabla \cdot \mathcal{D}} | c' \mathbf{y} \rangle \mathcal{J} \rho^{c'}(\mathbf{y}) d\mathbf{x} d\mathbf{y} . \end{aligned} \quad (1)$$

Here,  $\mathbf{\Pi}^{tr}$  and  $\mathcal{B}$  are the transverse chromo-electromagnetic fields in the QCD Coulomb gauge and  $\psi$  represents the quark fields. The last two terms in Eq. (1) are the quark-gluon interaction ( $g$ -term) and the total color-charge density interaction ( $g^2$ -term), respectively. In QCD, the total color-charge density  $\rho^c(\mathbf{x})$  contains the contribution of quarks-antiquarks and gluons. The kernel in the last term of Eq. (1) is the Instantaneous color-Coulomb Interaction in QCD (QCD-IcCI) which includes the inverse of the Faddeev-Popov operator  $(\nabla \cdot \mathcal{D})^{-1}$  and its determinant  $\mathcal{J} = \det(\nabla \cdot \mathcal{D})$  [9, 10]. At low energy, light quarks play the most important role, while the effects of dynamical gluons can be simulated by the interaction  $V(|\mathbf{x} - \mathbf{y}|) = -\frac{\alpha}{|\mathbf{x} - \mathbf{y}|} + \beta|\mathbf{x} - \mathbf{y}|$ , which is obtained from a self-consistent treatment of the interaction between color charge-densities [23, 28].

Therefore, an approximate effective QCD Hamiltonian can be written as

$$\begin{aligned} \mathbf{H}_{eff}^{QCD} &= \int \left\{ \psi^\dagger(\mathbf{x})(-i\boldsymbol{\alpha} \cdot \boldsymbol{\nabla} + \beta m)\psi(\mathbf{x}) \right\} d\mathbf{x} - \frac{1}{2} \int \rho_c(\mathbf{x})V(|\mathbf{x} - \mathbf{y}|)\rho^c(\mathbf{y})d\mathbf{x}d\mathbf{y} \\ &= \mathbf{K} + \mathbf{H}_{\text{Coul}} , \end{aligned} \quad (2)$$

where we have restricted ourselves to the quark sector of the theory, without dynamical gluons. Consequently,  $\rho^c(\mathbf{x}) = \psi^\dagger(\mathbf{x})T^c\psi(\mathbf{x})$  now represents the quark and antiquark charge density. In the last line of Eq. (2), the first term is the kinetic energy, while the second term is the QCD-IcCI in its simplified form. The reason for the factor of  $-\frac{1}{2}$  in the potential term is that the short-range interaction of two quarks with opposite (color) charges is similar to the classical attractive Coulomb interaction, i.e.,  $-\frac{q^2}{r}$  [13, 30]. The fields  $\psi^\dagger(\mathbf{x})$  and its hermitian conjugate are quantized in the usual way, by expanding them in terms of creation and annihilation operators and using as coefficients the harmonic oscillator functions:

$$\begin{aligned} \psi^\dagger(\mathbf{x}) &= \sum_{\tau, Nlm_i, \sigma cf} R_{Nl}^*(x)Y_{lm_i}^*(\hat{\mathbf{x}})\chi_\sigma^\dagger \mathbf{q}_{\tau, Nlm_i, \sigma cf}^\dagger \\ &= \sum_{Nlm_i, \sigma cf} R_{Nl}^*(x)Y_{lm_i}^*(\hat{\mathbf{x}})\chi_\sigma^\dagger \left( \mathbf{q}_{\frac{1}{2}, Nlm_i, \sigma cf}^\dagger + \mathbf{q}_{-\frac{1}{2}, Nlm_i, \sigma cf}^\dagger \right) . \end{aligned} \quad (3)$$

with  $x = |\mathbf{x}|$  and  $R_{Nl}(x) = N_{Nl} \exp(-\frac{B_0 x^2}{2}) x^l L_{\frac{N-l}{2}}^{l+\frac{1}{2}}(B_0 x^2)$ , where  $L_n^\lambda$  is an associated Laguerre polynomial and  $(\sqrt{B_0})^{-1}$  is the oscillator length. The index  $\tau$  denotes the upper ( $\tau = \frac{1}{2}$ ) and lower ( $\tau = -\frac{1}{2}$ ) components of the Dirac spinors in the Dirac-Pauli representation of the Dirac matrices, and  $\sigma, c, f$  indicate the spin, color and flavor intrinsic degrees of freedom, respectively.

For the implementation of the *Tamm-Dancoff Approximation* (TDA) and the *Random Phase Approximation* (RPA) methods in the present approach, we have developed the following strategy: in a first step, the kinetic energy term is diagonalized within a finite volume (Section II A), which we shall refer to as ‘‘prediagonalization’’. The eigenfunctions constitute a new basis, where quark and antiquark creation and annihilation operators can be defined. In a second step (Section II B), the interaction is rewritten in terms of these creation and annihilation operators. Finally, the whole Hamiltonian of Eq. (2), expressed in the effective basis, is diagonalized in the space of particle-hole collective states (Section III).

### A. Diagonalization of the kinetic energy and the effective basis.

The kinetic energy in terms of the creation and annihilation operators of the oscillator basis, in their total spin  $j = 1 + \frac{1}{2}$  representation, is written as

$$\mathbf{K} = \sum_{j\tau_i N l_i m c f} \sum_{\tau_1(N_1 l_1), \tau_2(N_2 l_2)} K_{\tau_1(N_1 l_1), \tau_2(N_2 l_2)}^{j, T} \mathbf{q}_{\tau_1(N_1 l_1) j m c f}^\dagger \mathbf{q}_{\tau_2(N_2 l_2) j m c f} \quad , \quad (4)$$

which is clearly not diagonal. The indices  $m, c$  and  $f$  correspond to the total spin  $m = -j, \dots, j$ , color  $c = 1, 2, 3$  and flavor  $f = u, d, s$  components, respectively, where  $f = \{Y, T, T_z\}$  is a short-hand notation for flavor-hypercharge, isospin and the third component of isospin. We distinguish between the u-d quarks ( $T = \frac{1}{2}$ ) and the s quarks ( $T = 0$ ), where the latter have a larger mass. The prediagonalization has to be applied in each sector with a different mass or isospin i.e.,  $m_0^T = m_{u,d}\delta_{T, \frac{1}{2}} + m_s\delta_{T, 0}$ . The matrix  $K_{\tau_1(N_1 l_1), \tau_2(N_2 l_2)}^{j, T}$  (given explicitly in Appendix A) has to be diagonalized in order to obtain an effective basis with respect to which the total Hamiltonian is then diagonalized.

The diagonalization of the kinetic term (4) is performed for a given maximal number of quanta  $N = N_{\text{cut}}$ , for which we introduce a general transformation to a basis of effective operators,

$$\mathbf{q}_{\tau(Nl) j m c f}^\dagger = \sum_{\lambda \pi k} \left( \alpha_{\tau(Nl), \lambda \pi k}^{j, T} \right)^* \mathbf{Q}_{\lambda \pi k j m c f}^\dagger \delta_{\pi, (-1)^{\frac{1}{2} - \tau + l}} \quad . \quad (5)$$

The index  $\lambda = \pm\frac{1}{2}$  refers to the pseudo-spin components after the diagonalization of the kinetic term, and  $k$  runs over all orbital states after the diagonalization. The value  $\lambda = +\frac{1}{2}$  refers to positive energy states (effective quarks) and the value  $\lambda = -\frac{1}{2}$  to negative energy states (effective antiquarks). For example, taking  $N_{\text{cut}} = 3$  and  $j = \frac{1}{2}$ , only the lowest two  $s$  and  $p$  orbital states contribute, so that the index for the positive energy states runs from  $k = 1$  to 2, for a fixed  $\tau$ . The same happens for the negative energy states. The parity on the left-hand side (L.H.S) in (5)

is given by  $(-1)^{\frac{1}{2}-\tau+l}$  while for the right-hand side (R.H.S.)  $\pi$  indicates the parity after the diagonalization *i.e.*, our effective particles ( $\mathbf{Q}_{\lambda\pi k_j m_c f}^\dagger$ ) are a linear combination of states with the same well-defined parity. The transformation coefficients depend on the type of quarks, whether it is an up or down quark (equal masses are assumed) or a strange quark ( $m_{u,d} < m_s$ ). For the transformation coefficients and the kinetic matrix elements, only the dependence on the flavor isospin is given, because the flavor-hypercharge is fixed by  $T$ .

The eigenvalue problem to be solved acquires the following form

$$\sum_{\tau_i N_i l_i} \alpha_{\tau_i, (N_i l_i), \lambda_1 \pi_1 k_1}^{j, T} K_{\tau_i (N_i l_i), \tau_2 (N_2 l_2)}^{j, T} \alpha_{\tau_2, (N_2 l_2), \lambda_2 \pi_2 k_2}^{j, T} = \varepsilon_{\lambda_1 \pi_1 k_1 j Y T} \delta_{\lambda_1 \lambda_2} \delta_{\pi_1 \pi_2} \delta_{k_1 k_2}, \quad (6)$$

where we have taken the transformation coefficients of Eq. (5) to be real.

It is worth mentioning that the spin, color and flavor quantum numbers of the single particles are conserved in the prediagonalization. In this work, we only consider single particles with total spin  $j = \frac{1}{2}$  in order to study low energy states built by pairs coupled to spin  $J = 0, 1$  and leave for future work the analysis of the contributions due to single particle spin  $j = \frac{3}{2}$ . The method presented here can directly be extended to  $j > \frac{1}{2}$ .

Having performed the diagonalization of Eq. (4), the kinetic energy is rewritten in terms of effective creation (annihilation) operators of quarks  $\mathbf{b}^\dagger(\mathbf{b})$  and antiquarks  $\mathbf{d}^\dagger(\mathbf{d})$  (see Appendix A),

$$\mathbf{K} = \sum_{\pi k j Y T} \varepsilon_{\pi k j Y T} \sum_{m c T_z} \left( \mathbf{b}_{\pi k j Y T, m c T_z}^\dagger \mathbf{b}^{\pi k j Y T, m c T_z} - \mathbf{d}^{\pi k j Y T, m c T_z} \mathbf{d}_{\pi k j Y T, m c T_z}^\dagger \right), \quad (7)$$

where the eigenvalues (effective masses) are denoted by  $\varepsilon_{\pi k j Y T}$  and the quark and antiquark operators are related to the operators before the prediagonalization via  $\mathbf{Q}_{\frac{1}{2}\pi k_j m_c f}^\dagger \rightarrow \mathbf{b}_{\pi k j Y T, m c T_z}^\dagger$  and  $\mathbf{Q}_{-\frac{1}{2}\pi k_j m_c f} \rightarrow \mathbf{d}_{\pi k j Y T, m c T_z}$  (see (A5)).

The diagonalization is achieved by choosing the oscillator length  $(\sqrt{B_0})^{-1}$  in such a way that for a given cut-off  $N_{\text{cut}} = N_0$  (called the *renormalization point*, see Appendix E) the first ( $k = 1$ ) single-particle state  $\varepsilon_{\pi k j Y T}$  is at a fixed energy. This energy is chosen such that it represents a confined particle in a finite volume of the size of a hadron, *i.e.*,  $0.5\text{fm} \leq (\sqrt{B_0})^{-1} \leq 1\text{fm}$ . The renormalization of the masses is explained in the Section III B and in the Appendix E.

## B. The effective Coulomb Interaction

In terms of the creation  $\mathbf{q}_{\tau(N_l)j m_c f}^\dagger$  and annihilation  $\mathbf{q}^{\tau(N_l)j m_c f}$  operators, before the prediagonalization, the effective Coulomb interaction acquires the form (see Appendix B)

$$\mathbf{H}_{\text{Coul}} = -\frac{1}{2} \sum_{N_i l_i j_i L} V_{\{N_i l_i j_i\}}^L \left[ \left[ \mathbf{q}_{(N_1 l_1) j_1}^\dagger \otimes \mathbf{q}_{(N_2 l_2) j_2} \right]^{0, L, (11), (00)} \otimes \left[ \mathbf{q}_{(N_3 l_3) j_3}^\dagger \otimes \mathbf{q}_{(N_4 l_4) j_4} \right]^{0, L, (11), (00)} \right]_{0, 0, 0, 0}^{0, 0, (00), (00)}, \quad (8)$$

The intermediate coupling refers to pseudo-spin zero, angular momentum  $L$ , color (1,1) and flavor (0,0), respectively. Since the TDA and RPA meson-like pairs will not be coupled to a definite  $SU(3)$  flavor irrep but only to a definite  $Y, T, T_z$ , it is preferable to rewrite the product  $\left[ \mathbf{q}_{(N_1 l_1) j_1}^\dagger \otimes \mathbf{q}_{(N_2 l_2) j_2} \right]_{0, M_L, C, 0}^{0, L, (11), (00)}$  as

$$\left[ \mathbf{q}_{(N_1 l_1) j_1}^\dagger \otimes \mathbf{q}_{(N_2 l_2) j_2} \right]_{0, M_L, C, 0}^{0, L, (11), (00)} = \sum_{Y_1 T_1, Y_2 T_2} (-1)^{\frac{1}{3} + \frac{Y_1}{2} + T_1} \frac{\sqrt{2T_1 + 1}}{\sqrt{3}} \delta_{T_2 T_1} \delta_{Y_2 Y_1} \left[ \mathbf{q}_{(N_1 l_1) j_1 Y_1 T_1}^\dagger \otimes \mathbf{q}_{(N_2 l_2) j_2 Y_2 T_2} \right]_{0, M_L, C, 0}^{0, L, (11), 00}, \quad (9)$$

where  $\bar{Y}_2 = -Y_2$  and the new factor in the sum comes from an isoscalar factor of  $SU(3)$  [31]. The last two zeros in the final coupling indices refer to  $Y$  and  $T$  while the (last) lower magnetic quantum number index refers to  $T_z$ .

Applying the transformation (5), the product of a creation and an annihilation operator in (9) transforms to

$$\begin{aligned} & \left[ \mathbf{q}_{(N_1 l_1) j_1 Y_1 T_1}^\dagger \otimes \mathbf{q}_{(N_2 l_2) j_2 \bar{Y}_2 T_2} \right]_{0, M_L, C, 0}^{0, L, (11), 00} \\ &= \frac{1}{\sqrt{2}} \sum_{\tau_1, \tau_2} \sum_{\lambda_1 \pi_1 k_1, \lambda_2 \pi_2 k_2} \delta_{\tau_1, \tau_2} \delta_{\pi_1, (-1)^{\frac{1}{2}-\tau_1+l_1}} \delta_{\pi_2, (-1)^{\frac{1}{2}-\tau_2+l_2}} \left( \alpha_{\tau_1 (N_1 l_1), \lambda_1 \pi_1 k_1}^{j_1, T_1} \right) \left( \alpha_{\tau_2 (N_2 l_2), \lambda_2 \pi_2 k_2}^{j_2, T_2} \right) \\ & \times \left\{ \delta_{\lambda_1, \frac{1}{2}} \delta_{\lambda_2, \frac{1}{2}} \left[ \mathbf{b}_{\pi_1 k_1 j_1 Y_1 T_1}^\dagger \otimes \mathbf{b}_{\pi_2 k_2 j_2 \bar{Y}_2 T_2} \right]_{M_L, C, 0}^{L, (11), 00} - \delta_{\lambda_1, \frac{1}{2}} \delta_{\lambda_2, -\frac{1}{2}} \left[ \mathbf{b}_{\pi_1 k_1 j_1 Y_1 T_1}^\dagger \otimes \mathbf{d}_{\pi_2 k_2 j_2 \bar{Y}_2 T_2}^\dagger \right]_{M_L, C, 0}^{L, (11), 00} \right. \\ & \left. + \delta_{\lambda_1, -\frac{1}{2}} \delta_{\lambda_2, \frac{1}{2}} \left[ \mathbf{d}_{\pi_1 k_1 j_1 Y_1 T_1} \otimes \mathbf{b}_{\pi_2 k_2 j_2 \bar{Y}_2 T_2} \right]_{M_L, C, 0}^{L, (11), 00} - \delta_{\lambda_1, -\frac{1}{2}} \delta_{\lambda_2, -\frac{1}{2}} \left[ \mathbf{d}_{\pi_1 k_1 j_1 Y_1 T_1} \otimes \mathbf{d}_{\pi_2 k_2 j_2 \bar{Y}_2 T_2}^\dagger \right]_{M_L, C, 0}^{L, (11), 00} \right\}. \quad (10) \end{aligned}$$

This allows us to introduce the following notation

$$\begin{aligned} \mathcal{F}_{1,2; \Gamma_0, \mu_0} &= \frac{1}{\sqrt{2}} \left\{ \delta_{\lambda_1, \frac{1}{2}} \delta_{\lambda_2, \frac{1}{2}} \left[ \mathbf{b}_{\pi_1 k_1 j_1 Y_1 T_1}^\dagger \otimes \mathbf{b}_{\pi_2 k_2 j_2 Y_2 T_2} \right]_{M_L, C, 0}^{L, (11), 00} - \delta_{\lambda_1, -\frac{1}{2}} \delta_{\lambda_2, -\frac{1}{2}} \left[ \mathbf{d}_{\pi_1 k_1 j_1 Y_1 T_1} \otimes \mathbf{d}_{\pi_2 k_2 j_2 Y_2 T_2}^\dagger \right]_{M_L, C, 0}^{L, (11), 00} \right\} \\ \mathcal{G}_{1,2; \Gamma_0, \mu_0} &= \frac{1}{\sqrt{2}} \left\{ \delta_{\lambda_1, -\frac{1}{2}} \delta_{\lambda_2, \frac{1}{2}} \left[ \mathbf{d}_{\pi_1 k_1 j_1 Y_1 T_1} \otimes \mathbf{b}_{\pi_2 k_2 j_2 Y_2 T_2} \right]_{M_L, C, 0}^{L, (11), 00} - \delta_{\lambda_1, \frac{1}{2}} \delta_{\lambda_2, -\frac{1}{2}} \left[ \mathbf{b}_{\pi_1 k_1 j_1 Y_1 T_1}^\dagger \otimes \mathbf{d}_{\pi_2 k_2 j_2 Y_2 T_2}^\dagger \right]_{M_L, C, 0}^{L, (11), 00} \right\}. \end{aligned} \quad (11)$$

where we have used the short-hand notations  $1 = \lambda_1 \pi_1 k_1 j_1 Y_1 T_1$  (similarly for the index 2), for the quantum numbers of the intermediate coupling in the interaction  $\Gamma_0 = L, (11), 00$ , and for their magnetic projections  $\mu_0 = M_L, C, 0$ , respectively.

With this, the Coulomb interaction is rewritten as

$$\mathbf{H}_{Coul} = -\frac{1}{2} \sum_L \sum_{\lambda_i \pi_i k_i j_i Y_i T_i} V_{\{\lambda_i \pi_i k_i j_i Y_i T_i\}}^L \left( [\mathcal{F}_{12; \Gamma_0} \mathcal{F}_{34; \bar{\Gamma}_0}]_{\bar{0}}^{\bar{0}} + [\mathcal{F}_{12; \Gamma_0} \mathcal{G}_{34; \bar{\Gamma}_0}]_{\bar{0}}^{\bar{0}} + [\mathcal{G}_{12; \Gamma_0} \mathcal{F}_{34; \bar{\Gamma}_0}]_{\bar{0}}^{\bar{0}} + [\mathcal{G}_{12; \Gamma_0} \mathcal{G}_{34; \bar{\Gamma}_0}]_{\bar{0}}^{\bar{0}} \right), \quad (12)$$

where the upper index  $\bar{0} = \{0, (00), 00\}$  indicates the total couplings of the interaction in spin, color and flavor hypercharge and isospin, while the lower index  $\bar{0} = \{0, 0, 0\}$  indicates the corresponding magnetic numbers.

The second and third terms in Eq. (12) do not contribute in either the TDA or the RPA scheme, since they have an odd number of creation and annihilation operators. They can eventually be absorbed in higher order terms of the coupling between quarks, antiquarks and phonons. The creation and annihilation of two pairs, contained in the last term of Eq. (12), only contributes in the RPA scheme and accounts for the presence of ground state correlations in this framework.

The matrix elements in Eq. (12) are given by

$$\begin{aligned} V_{\{\lambda_i \pi_i k_i j_i Y_i T_i\}}^L &= \sum_{\tau_i N_i l_i} V_{\{N_i l_i j_i\}}^L \alpha_{\tau_1(N_1 l_1), \lambda_1, \pi_1, k_1}^{j_1, T_1} \alpha_{\tau_2(N_2 l_2), \lambda_2, \pi_2, k_2}^{j_2, T_2} \alpha_{\tau_3(N_3 l_3), \lambda_3, \pi_3, k_3}^{j_3, T_3} \alpha_{\tau_4(N_4 l_4), \lambda_4, \pi_4, k_4}^{j_4, T_4} \\ &\times \delta_{\tau_1 \tau_2} \delta_{\tau_3 \tau_4} \delta_{\pi_1, (-1)^{\frac{1}{2} - \tau_1 + l_1}} \delta_{\pi_2, (-1)^{\frac{1}{2} - \tau_2 + l_2}} \delta_{\pi_3, (-1)^{\frac{1}{2} - \tau_3 + l_3}} \delta_{\pi_4, (-1)^{\frac{1}{2} - \tau_4 + l_4}} \\ &\times (-1)^{\frac{1}{3} + \frac{Y_1}{2} + T_1} \frac{\sqrt{2T_1 + 1}}{\sqrt{3}} \delta_{T_2 T_1} \delta_{Y_2 Y_1} (-1)^{\frac{1}{3} + \frac{Y_3}{2} + T_3} \frac{\sqrt{2T_3 + 1}}{\sqrt{3}} \delta_{T_4 T_3} \delta_{Y_4 Y_3}, \end{aligned} \quad (13)$$

and the matrix elements in the harmonic oscillator basis ( $V_{\{N_i l_i j_i\}}^L$ ) are analytic and actually easy to compute. They are given in Appendix B.

### III. THE TDA AND RPA BOSONIZATION METHODS.

The TDA and RPA are both bosonization (or linearization) methods [32]. In Appendix C, we present a brief introduction to the RPA method and its simplified TDA limit. The quark-antiquark pair operators needed for the TDA and RPA one phonon states with quantum numbers  $\Gamma = \{J^P, (0, 0)_C, Y, T\}$  and magnetic projection numbers  $\mu = \{M_j, 0, T_z\}$  are given by

$$[\mathbf{b}_{\pi_a k_a j_a Y_a T_a}^\dagger \otimes \mathbf{d}_{\pi_b k_b j_b Y_b T_b}^\dagger]_{M_j, 0, T_z}^{J^P, (0, 0)_C, Y, T} = [\mathbf{b}_a^\dagger \mathbf{d}_b^\dagger]_{\mu}^{\Gamma}, \quad (14)$$

where the creation (annihilation) operators of effective particles  $\mathbf{b}_{\pi_i k_i j_i m_i c_i f_i}^\dagger$  ( $\mathbf{b}^{\pi_i k_i j_i m_i c_i f_i}$ ) and antiparticles  $\mathbf{d}^{\pi_i k_i j_i m_i c_i f_i}$  ( $\mathbf{d}_{\pi_i k_i j_i m_i c_i f_i}$ ) were introduced in the previous Section. On the R.H.S. of Eq. (14) we have introduced the short-hand notation that we are going to use from now on, in order to describe all possible pairs needed to construct the collective TDA and RPA phonon operators.

Here, we present the more general phonon operators that we are going to implement, *i.e.*, the RPA creation phonon operators  $\hat{\Gamma}_{n; \Gamma \mu}^\dagger$ , which are defined as

$$\begin{aligned} \hat{\Gamma}_{n; \Gamma \mu}^\dagger &= \sum_{\mathbf{a}, \mathbf{b}} \left\{ X_{\mathbf{ab}; \Gamma}^n [\mathbf{b}_a^\dagger \mathbf{d}_b^\dagger]_{\mu}^{\Gamma} - Y_{\mathbf{ab}; \Gamma}^n (-1)^{\phi_{\Gamma \mu}} [\mathbf{d}^{\bar{\mathbf{b}}} \mathbf{b}^{\bar{\mathbf{a}}}]_{\bar{\mu}}^{\bar{\Gamma}} \right\} \\ &= \sum_{\mathbf{a}, \mu_a} \sum_{\mathbf{b}, \mu_b} \left\{ X_{\mathbf{ab}; \Gamma}^n \langle \mathbf{a} \mu_a, \bar{\mathbf{b}} \bar{\mu}_b | \Gamma \mu \rangle \mathbf{b}_{\mathbf{a} \mu_a}^\dagger \mathbf{d}_{\bar{\mathbf{b}} \bar{\mu}_b}^\dagger - Y_{\mathbf{ab}; \Gamma}^n (-1)^{\phi_{\Gamma \mu}} \langle \mathbf{a} \mu_a, \bar{\mathbf{b}} \bar{\mu}_b | \bar{\Gamma} \bar{\mu} \rangle \mathbf{d}^{\bar{\mathbf{b}} \bar{\mu}_b} \mathbf{b}^{\mathbf{a} \mu_a} \right\} \end{aligned} \quad (15)$$

where  $(-1)^{\phi_{\Gamma\mu}} = (-1)^{J-M_J}(-1)^{T-T_z}$  is the phase needed to guarantee the scalar nature of the vacuum.

The corresponding annihilation phonon operators  $\hat{\Gamma}^{n;\Gamma\mu}$  are

$$\begin{aligned}\hat{\Gamma}^{n;\Gamma\mu} &= \sum_{\mathbf{a},\mathbf{b}} \left\{ (X_{\mathbf{ab};\Gamma}^n)^* [d^{\bar{\mathbf{b}}}\mathbf{b}^{\mathbf{a}}]_{\mu}^{\Gamma} - (Y_{\mathbf{ab};\Gamma}^n)^* (-1)^{\phi_{\Gamma\mu}} [b_{\mathbf{a}}^{\dagger}d_{\bar{\mathbf{b}}}^{\dagger}]_{\bar{\mu}}^{\bar{\Gamma}} \right\} \\ &= \sum_{\mathbf{a},\mu_{\mathbf{a}}} \sum_{\mathbf{b},\mu_{\mathbf{b}}} \left\{ (X_{\mathbf{ab};\Gamma}^n)^* \langle \mathbf{a}\mu_{\mathbf{a}}, \bar{\mathbf{b}}\bar{\mu}_{\mathbf{b}} | \Gamma\mu \rangle d^{\bar{\mathbf{b}}\bar{\mu}_{\mathbf{b}}} \mathbf{b}^{\mathbf{a}\mu_{\mathbf{a}}} - (Y_{\mathbf{ab};\Gamma}^n)^* (-1)^{\phi_{\Gamma\mu}} \langle \mathbf{a}\mu_{\mathbf{a}}, \bar{\mathbf{b}}\bar{\mu}_{\mathbf{b}} | \bar{\Gamma}\bar{\mu} \rangle b_{\mathbf{a}\mu_{\mathbf{a}}}^{\dagger} d_{\bar{\mathbf{b}}\bar{\mu}_{\mathbf{b}}}^{\dagger} \right\}, \quad (16)\end{aligned}$$

where  $\mathbf{a} = \pi_a, k_a, j_a, Y_a, T_a$  ( $\bar{\mathbf{b}} = \pi_b, k_b, j_b, -Y_b, T_b$ ) and  $\mu_{\mathbf{a}} = m_a c_a T_{az}$  ( $\bar{\mu}_{\mathbf{b}} = -m_b \bar{c}_b - T_{bz}$ ) are the irreducible representations and the third components of quarks (antiquarks), respectively, while  $\langle \mathbf{a}\mu_{\mathbf{a}}, \bar{\mathbf{b}}\bar{\mu}_{\mathbf{b}} | \Gamma\mu \rangle$  is a short-hand notation for the product over all Clebsch-Gordan coefficients involved (spin, color and flavor). The quantities  $X_{\mathbf{ab};\Gamma}^n$  are the *forward-going-amplitudes* and  $Y_{\mathbf{ab};\Gamma}^n$  are the *backward-going-amplitudes*. The TDA limit is obtained when the backward-going-amplitudes  $Y_{\mathbf{ab};\Gamma}^n$  are set to zero. All the details about the phonon operators and the implementation of the TDA and RPA methods are presented in Appendix C.

Before discussing our TDA and RPA results, we describe our general procedure for the numerical calculations:

- We are not considering dynamical gluons, but their main effects are accounted for by an effective confining potential, obtained from a self-consistent treatment (Dyson-Schwinger equations) of the Yang-Mills degrees of freedom in the presence of static quarks [23].
- For the fermion fields, we implement the canonical quantization in terms of a basis of wave functions and the corresponding creation (annihilation) operators, see Eq. (3). In particular, we have chosen the harmonic oscillator basis for the expansion of the fermion fields and used it to exactly diagonalize the kinetic Dirac term (see Section II A) in each flavor-isospin sector, in order to obtain effective quarks and antiquarks.
- Then, the effective QCD Hamiltonian has a diagonal single-particle term representing the kinetic energies (including the masses) of the effective quarks (Eq. (7)), while now the matrix elements of the color Coulomb confining interaction  $\mathbf{H}_{\text{Coul}}$  are not only spin and color dependent but also flavor-isospin dependent, as shown in Eq. (13), as a consequence of the unitary transformation  $\alpha_{\tau,(NI);\lambda\pi,k}^{j,T}$ .
- It is reasonable to expect that the masses of the effective up, down and strange quarks are higher than the corresponding current quark masses, and different from each other. These differences account for the effects of the chiral and flavor symmetry breaking and they are represented by the unitary transformation of Eq. (5). Here, we consider that the current strange quarks have a higher mass than the up and down quarks. For simplicity, we use up and down quarks with the same mass, *i.e.*,  $m_s > m_{u,d}$ . We are then in a position to describe the interaction of the effective up, down and strange quarks at low energies.
- In order to study the predictive power of our approach, the numerical calculations are restricted first to a particle-hole space by means of the TDA where the  $1p - 1h$  correlations are only taken into account in the excited states, keeping the ground state unchanged. This allows us to give a quantitative analysis of the ground state correlations once the RPA method is implemented. The collective TDA eigenstates are compared to experimental data in the subspaces of spin, parity, color, flavor-hypercharge and isospin quantum numbers  $\{J^P, (0,0)_C, (Y,T)\}$  for masses up to 1 GeV, with  $J^P = 0^{\mp}, 1^{-}$  and  $(Y,T) = (\pm 1, \frac{1}{2}), (0,0), (0,1)$ .
- In a further step, we include also ground state  $p - h$  correlations by means of the RPA within the same subspaces  $\{J^P, (0,0)_C, (Y,T)\}$ . By exploring the influence of ground state correlations in a comparison of the RPA-phonon eigenvalues with the corresponding TDA eigenvalues and the experimental data, we obtain insights into the physics around the pion state, as well as a look at the controversial scalar mesons ( $J^P = 0^+$ ).
- Finally, to absorb any dependence of the configurational space on the cut-off  $N_{\text{cut}}$ , we have to implement a renormalization procedure. We will require that the observables are weakly depending on the cut-off of the configurational space. To achieve this, the effective particle energies obtained from the prediagonalization of the kinetic energy term also have to be independent of the cut-off, while the bare quark masses ( $m_{u,d}$  and  $m_s$ ) and the interaction parameters (couplings  $\alpha$  and  $\beta$ ) get renormalized as functions of  $N_{\text{cut}}$ . The details of the renormalization procedure are shown in Appendix E.



### A. TDA and RPA results

In what follows, we present our results and compare them with the results obtained in [29] and with the experimental data [33]. We also compare the TDA and RPA results with each other in order to explore the influence of the ground state correlations in the different subspaces  $\{J^P, (0,0)_C, (Y,T)\}$  where both methods are implemented. From now on, we are going to omit the singlet color notation  $(0,0)_C$  from the TDA and RPA subspaces of diagonalization, since by construction all the collective TDA and RPA states presented here are color singlet.

In order to grasp the main features of the low-energy sector of the meson spectrum, it is worth to mention the isospin, spin and parity  $T(J^P)$  quantum numbers of the states up to about 1 GeV [33]. For the pseudoscalar mesons: the pion state has  $T(J^P) = 1(0^-)$ , the charged  $K^\pm$  and neutral kaons  $K^0$  have  $T(J^P) = \frac{1}{2}(0^-)$ , and the  $\eta, \eta'$  mesons have  $T(J^P) = 0(0^-)$ . For the vector mesons: the  $\rho$  meson has  $T(J^P) = 1(1^-)$ , the vector kaon states have  $T(J^P) = \frac{1}{2}(1^-)$ , while both the  $\omega$  and  $\phi$  mesons have  $T(J^P) = 0(1^-)$ . For the scalar mesons: the  $a_0$  meson has  $T(J^P) = 1(0^+)$ , the  $K_0^*$  has  $T(J^P) = \frac{1}{2}(0^+)$ , and the  $f_0(500), f_0(980) = f_0^*$  mesons both have  $T(J^P) = 0(0^+)$ . There is no pseudovector meson reported below 1 GeV [33].

The TDA and RPA eigenstates in the  $\{J^P, (Y,T)\} = \{J^P, (0,0)\}$  subspaces show only pure  $q\bar{q}$  ( $q = u, d$ ) and  $s\bar{s}$  states, *i.e.*, no flavor mixing. The reason for such pure states is the fact that the effective color-confining interaction is not capable to produce flavor mixing between pairs, as a consequence of the color structure of the quark (antiquark) color-charge densities  $\rho^a$ , which are flavor scalars (see Eq. (13)). Flavor mixing is expected to occur, however, in the meson spectrum, *e.g.*, for the  $T(J^P) = 0, (0^-)$   $\eta$  and  $\eta'$  physical states. In the present approach, then, the  $\eta$  and  $\eta'$  states will be described by pure  $q\bar{q}$  and  $s\bar{s}$  collective TDA and RPA states. However, we will explore a flavor mixing procedure, following [34], in the subspace  $\{0^-, (0,0)\}$ , *i.e.*, for pseudoscalar  $\eta, \eta'$  states. In the case of the  $\omega, \phi$  and  $f_0$  mesons, related to the subspaces  $\{1^-, (0,0)\}$  and  $\{0^+, (0,0)\}$ , respectively, the more common description of these states in the literature is as pure flavorless states.

For the TDA and RPA results presented here, we have used  $N_{\text{cut}} = N_0 = 3$  (the renormalization procedure for higher  $N_{\text{cut}}$  is shown in Section IIIB and Appendix E). In Table I, we show the values of the quark masses and interaction parameters used in both calculations. For a quantitative evaluation of the importance of the Coulomb potential  $\frac{\alpha}{|\mathbf{x}-\mathbf{y}|}$  (not considered in [29]) with respect to the linear potential  $\beta|\mathbf{x}-\mathbf{y}|$ , we also compare the results of the calculations with  $\alpha = 0$  to those with  $\alpha \neq 0$ .

For  $N_{\text{cut}} = N_0 = 3$ , we fit the parameters of the model in such a way that the RPA calculation reproduces the pion mass (139 MeV) as close as possible, while the rest of the RPA spectrum (*i.e.*, pseudoscalar, vector and scalar mesons) is a consequence of this fit.

Set \ parameters	$m_{u,d}[GeV]$	$m_s[GeV]$	$\alpha$	$\beta[GeV^2]$
1	0.05	0.31	0.0	0.40
2	0.05	0.31	0.16	0.40

TABLE I: Parameters  $\alpha$  and  $\beta$  of the interaction  $V(|\mathbf{x}-\mathbf{y}|)$  and the masses of the u,d and s quarks, used for the TDA and RPA calculations. We have set the harmonic oscillator length to  $1/\sqrt{B_0} = 0.75\text{fm}$ .

We shall now briefly comment on the determination of the C-parity of the states under consideration. Given that we restrict our calculations to the  $j = \frac{1}{2}$  sector of the basis, the orbital angular momentum for each quark can only be zero or one. Thus, in the relative motion (see Appendix B), the two orbital angular momenta can only couple to the total relative orbital angular momentum  $l_r = 0, 1$  or  $2$ . The spin  $S$  of the quark-antiquark pair can be zero or one, so that the possible values of the total spin  $J$  are  $J = l_r \pm 1$  and  $J = l_r$  for  $S = 1$ , and  $J = l_r$  for  $S = 0$ . The parity of a state is given by  $P = -(-1)^{l_r}$ , where the extra minus sign is due to the relative intrinsic parities of the quark and antiquark. In particular, when  $J$  and  $P$  are defined, one also knows whether  $J = l_r$  or  $J = l_r \pm 1$ . When one applies the charge conjugation operator to, for example, a  $u\bar{u}$  state, one obtains  $\bar{u}u$ . In order to relate the latter state to the former, one has to exchange the two fermions (giving a factor  $(-1)$ ), including their positions ( $(-1)^{l_r}$ ) and their spins (a factor of  $-(-1)^S$ ). The eigenvalue  $C$  is the product of these factors, giving  $C = (-1)^{l_r+S}$ . With this, we can deduce the C-parity of the states of interest:

- i) Pseudoscalars,  $J^P = 0^-$ : This implies that  $l_r$  is even, *i.e.*, that  $l_r$  is zero, because for  $l_r = 2$ , and considering that the spin can maximally be one, the value  $J = 0$  cannot be reached. Then  $S$  has to be zero, too, because  $l_r = 0$  and  $S = 1$  would give  $J = 1$ . When  $l_r = S = 0$ , the C-parity is positive.
- ii) Vector mesons,  $J^P = 1^-$ : Because of the negative parity,  $l_r$  has to be even, *i.e.*,  $l_r$  is 0 or 2. In both cases,  $S$  has

to be one in order to get  $J = 1$ , hence  $C = -$ .

iii) Scalars,  $J^P = 0^+$ : Because  $P$  is positive,  $l_r$  has to be odd. It follows that  $l_r = 1$  and  $S = 1$ , *i.e.*,  $C = +$ .

### Pseudoscalar mesons.

For the pseudoscalar mesons four diagonalizations are involved, one for each subspace  $(Y, T)$ , however, the sectors  $(\pm 1, \frac{1}{2})$  exhibit the expected degeneracy and the number of diagonalizations can be reduced to three. Since we are not making any distinction at the moment between charged and neutral mesons, we report one pion- and one kaon-like state, corresponding to the lowest eigenvalue obtained for  $T = 1$  and  $T = \frac{1}{2}$ , respectively. The  $\eta$ - and  $\eta'$ -like states in Table II are pure  $q\bar{q}$  and  $s\bar{s}$  states respectively, *i.e.*, no flavor mixing [35, 36] has been implemented.

State	Exp.	TDA(Set1)	TDA(Set2)	RPA(Set1)	RPA(Set2)
$\pi$	139	249	245	145	136
K	495	468	465	468	465
$\eta$	547	249	245	145	136
$\eta'$	957	688	687	670	668

TABLE II: Experimental pseudoscalar meson masses [MeV] compared to both TDA and RPA results, for the parameters given in Table I.

From Table II, it can be seen that the  $T = 0$  and  $T = 1$  subspaces are affected by the influence of the ground state correlations, while the  $T = \frac{1}{2}$  subspace remains unchanged. In particular, the RPA pion-like state is improved with respect to the TDA one, and is in good agreement with the experimental value. The reported pseudoscalar kaon mass is well reproduced in this approach, contrary to the case of Ref. [29], see Figure 1.

In Table II, we show the results for the  $\eta$  and  $\eta'$  mesons as TDA and RPA collective states built from pure  $q\bar{q}$  and  $s\bar{s}$  states, respectively. As we have explained before, the interactions that are responsible for the mixing of the  $q\bar{q}$  and  $s\bar{s}$  states are missing in the effective Hamiltonian (2). A proper dynamical implementation of flavor mixing is beyond the purpose of the present work. Our pure  $q\bar{q}$  and  $s\bar{s}$  states, associated with the description of the  $\eta$  and  $\eta'$  states, share some similarities with the states obtained in Ref. [29] and are compared with the latter in Figure 1.

For the sake of completeness, we shall add a few more remarks on the issue of flavor mixing. In the presence of dynamical gluons, a color singlet quark-antiquark pair can be virtually annihilated into gluons which subsequently create a new color singlet quark-antiquark pair, not necessarily with the same flavor. In full QCD, a  $q\bar{q}$  state can thus be converted into a  $s\bar{s}$  state and vice versa. The same mechanism also produces  $q\bar{q}$  states from  $q\bar{q}$  states and  $s\bar{s}$  states from  $s\bar{s}$  states. The amplitudes for these virtual annihilation processes are approximately flavor-independent.

An effective description of flavor mixing in the subspace of the  $q\bar{q}$  and  $s\bar{s}$  states has been suggested a long time ago in Ref. [34]. In the present context, we would only include the first  $q\bar{q}$  and  $s\bar{s}$  states of the TDA or RPA solutions and consider them as a type of effective degrees of freedom. Notice that by doing so, we are clearly imposing a severe restriction, because if we preserve the TDA and RPA mappings from the quark-antiquark basis to the phonon basis, any sort of added interaction should affect all the solutions and not only the  $\eta$ - and  $\eta'$ -like solutions.

In its simplest form, the effective Hamiltonian restricted to the subspace of the (lowest-lying)  $q\bar{q}$  and  $s\bar{s}$  states is given by the  $2 \times 2$  matrix [29, 34]

$$\begin{pmatrix} M_{q\bar{q}} + 2H_{FM} & \sqrt{2} H_{FM} \\ \sqrt{2} H_{FM} & M_{s\bar{s}} + H_{FM} \end{pmatrix}. \quad (17)$$

The masses  $M_{q\bar{q}}$  and  $M_{s\bar{s}}$  in (17) correspond to the lowest, TDA or RPA,  $q\bar{q}$  and  $s\bar{s}$  eigenvalues of the Hamiltonian (2), in the subspace  $\{0^-, (0, 0)\}$ . Their values are shown in Table II. The parameter  $H_{FM}$  represents the flavor-independent amplitude of the virtual annihilation processes and will simply be adjusted to the data. The factors of two and  $\sqrt{2}$  multiplying  $H_{FM}$  are a consequence of the fact that we do not distinguish between  $u\bar{u}$  and  $d\bar{d}$  states in the present formulation. In this context, the  $q\bar{q}$  state is to be identified with the isospin singlet state  $|q\bar{q}\rangle = \frac{1}{\sqrt{2}}(|u\bar{u}\rangle + |d\bar{d}\rangle)$ . The eigenvalues of the flavor mixing matrix (17) are given by

$$E_{\pm} = \frac{1}{2} \left( M_{q\bar{q}} + M_{s\bar{s}} + 3H_{FM} \pm \sqrt{9H_{FM}^2 + 2H_{FM}(M_{q\bar{q}} - M_{s\bar{s}}) + (M_{q\bar{q}} - M_{s\bar{s}})^2} \right). \quad (18)$$

In Table III, we show the fit to the experimental masses, for both TDA and RPA frameworks, and the corresponding values of the phenomenological parameter  $H_{FM}$ .



State	Exp.	TDA(Set2)	$H_{FM}$	RPA(Set2)	$H_{FM}$
$\eta$	547	436	154	356	170
$\eta'$	957	958	154	958	170

TABLE III: Experimental and flavor-mixed TDA and RPA results, for the  $\eta$  and  $\eta'$  masses [MeV].

For a complete dynamical description of the flavor mixing processes in the Coulomb gauge formalism, dynamical gluon degrees of freedom would have to be included in the effective Hamiltonian (see Eq. (1)) to allow for transitions between quark-antiquark and multi-gluon states. Such an extension is left for future work.

### Vector mesons.

For the vector mesons calculated with the masses and coupling constants listed in Table I, we have obtained the TDA and RPA results shown in Table IV.

State	Exp.	TDA(Set1)	TDA(Set2)	RPA(Set1)	RPA(Set2)
$\rho$	770	688	687	677	676
$\omega$	782	688	687	677	676
$K^*$	892	941	942	941	942
$\phi$	1020	1144	1147	1142	1145

TABLE IV: Experimental vector meson masses [MeV] compared to both TDA and RPA results, for the parameters given in Table I.

The TDA and RPA eigenvalues are in good correspondence with the experimental data. The energy differences between the experimental vector masses and our TDA and RPA results are at about 5 – 12%. When assessing the success of the method, one should take the simplicity of the procedure and the low computational cost into account.

In Table IV, we show the results for the  $\omega$  and  $\phi$  mesons as TDA and RPA collective states built by pure  $q\bar{q}$  and  $s\bar{s}$  states, respectively. The latter is the most common description for these states in the literature. In [37], a flavor mixing mechanism was used to describe these states, the resulting mixing angle was very small, in agreement with the picture of pure states. In the present approach the effects of an additional interaction, similar to that described for the pseudoscalar states could yield a better agreement with the  $\rho$  and  $\phi$  experimental masses, but should be small.

In Figure 1, we show the RPA results obtained with the Set-2 of parameters, *i.e.*, the results that better reproduce the pion energy, compare them to the non-perturbative approach published in [29] and to the experimental values [33]. As can be seen from Figure 1, the experimental mass of the pseudoscalar kaon is well reproduced in the present approach, and much less satisfactorily so in [29]. In general, our results for the kaon-like states, for  $J^P = 0^-, 1^-$  (and  $0^+$ , see below), are in good correspondence with the experimental values, once the pion-like state is fitted

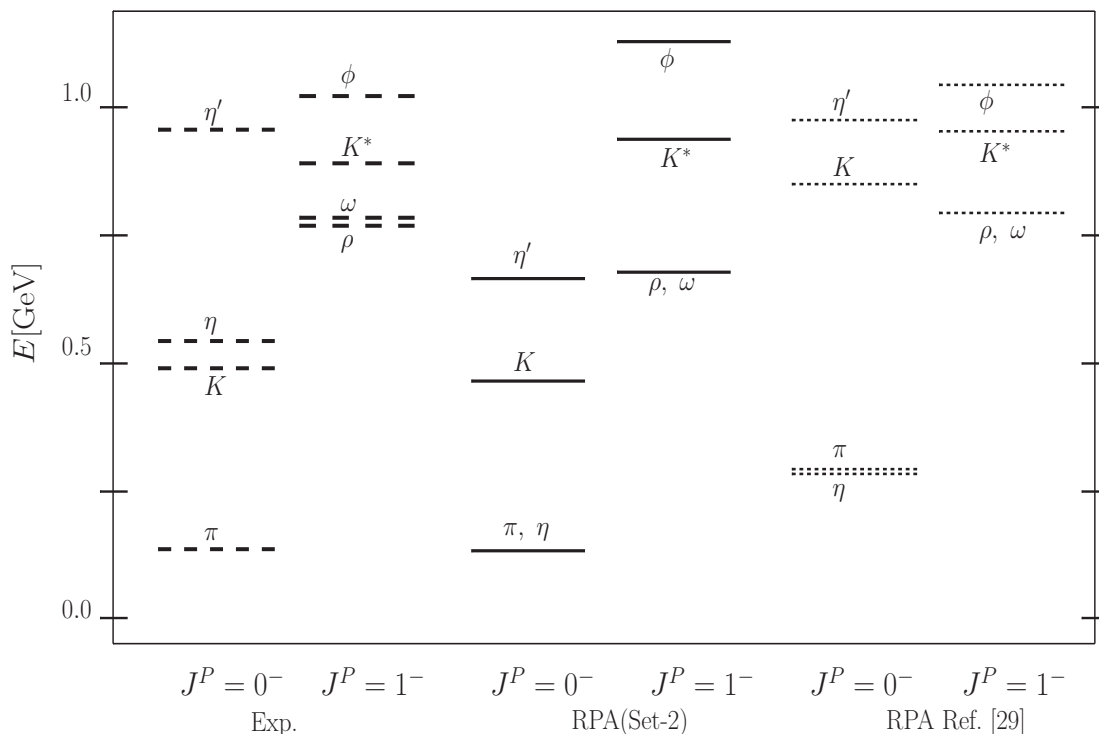


FIG. 1: RPA pseudoscalar and vector results of Set-2 compared with those obtained in Ref. [29] and with experimental data.

It is apparent from the results shown in Figure 1 that several features of the pseudoscalar and vector meson spectrum are reproduced, like those associated with the spin and flavor-isospin dependence, see also Tables II and IV. The energy difference between vector and pseudoscalar mesons with the same flavor-isospin (quark content) but different spin, like  $\rho$  and  $\pi$  or the  $K^*$  and  $K$  states, are reproduced satisfactorily, while the energy difference between mesons with the same spin but different flavor-isospin, like  $K$  and  $\pi$  or  $K^*$  and  $\rho$ , are reproduced acceptably. These spin and flavor-isospin dependence effects seem to be hidden in the QCD Hamiltonian of Eq. (1) as well as in the effective color-confining interaction of Eq. (2). The main differences between our calculated spectrum and the experimental one are in the  $\eta$  and  $\eta'$  sector.

### Scalar mesons.

We have performed the same analysis as for the pseudoscalar and vector states also for the scalar states. The scalar mesons below 1 GeV are very controversial [33, 38, 39], given that the scalar resonances are difficult to identify because some of them have large decay widths, which cause a strong overlap between resonances and background. However, a few scalar mesons are listed in the PDG [33]. Their quantum numbers  $T(J^P)$  and widths are: for the quantum numbers  $\frac{1}{2}(0^+)$ , the  $K_0^*(800)$  (or  $\kappa$ ) with a width of 547 MeV; for  $1(0^+)$ , the  $a_0(980)$  with a width of 50 – 100 MeV; and for  $0(0^+)$ , the  $f_0(500)$  (or  $\sigma$ ) with a width of 400 – 700 MeV and the  $f_0(980)$  with a width of 10 – 100 MeV.

In Table V, we present the scalar TDA and RPA results with masses approximately 1 GeV. In the subspace with  $(Y, T) = (0, 0)$ , the  $f_0(500)$  is the first TDA and RPA predicted pure  $q\bar{q}$  state, while the  $f_0(980)$  is the first predicted pure  $s\bar{s}$  state. In [40], the possibility that the  $f_0(500)$  and  $f_0(980)$  were related was analyzed. The reported mixing angle was about  $19^\circ$ . This picture is not that far from the pure  $q\bar{q}$  and  $s\bar{s}$  description presented in Table V. However, our TDA and RPA results indicate that a sizeable flavor mixing would be needed to arrive at a satisfactory description of the experimental  $f_0$  masses.

For the case of states with  $T = \frac{1}{2}$  and  $T = 1$  *i.e.*,  $K_0^*$  and  $a_0$ , respectively, we show in Table V the TDA and RPA results which are closest to the experimental values. The other states obtained in these subspaces with energies up to 1 GeV are discussed below.

State	Average	TDA(Set1)	TDA(Set2)	RPA(Set1)	RPA(Set2)
$f_0(500)$	(400-500)	259	256	154	145
$K_0^*(800)$	682	789	788	789	788
$f_0(980)$	990	701	700	684	683
$a_0(980)$	980	903,1001	910,1005	870,961	877,965

TABLE V: Experimental scalar meson masses in units of [MeV] [33], compared to both TDA and RPA results, for the Set-2 of parameters given in Table I. The average values are also taken from [33].

The average values given in Table V account for the large number of results reported in the literature.

It has been argued that the  $T(J^P) = 0(0^+)$ -states  $f_0(500)$  and  $f_0(980)$  have some similarities to the  $T(J^P) = 0(0^-)$ -states  $\eta(547)$  and  $\eta'(957)$ . Particularly, their reported masses are almost the same. In the present approach, although the TDA and RPA eigenvalues are lower than the experimental values, similarities in the masses between the pseudoscalar and scalar states belonging to the subspaces  $(Y, T) = (0, 0)$  are also observed in Tables II and V.

In [29], the reported TDA and RPA energy differences between the  $f_0$  states are 447 MeV and 513 MeV, respectively. In the present approach, the same differences, for the Set-2 of parameters of Table I, are 444 MeV and 538 MeV, respectively. These results are in good agreement with the energy difference between the experimental  $f_0$  masses, which is 480 MeV.

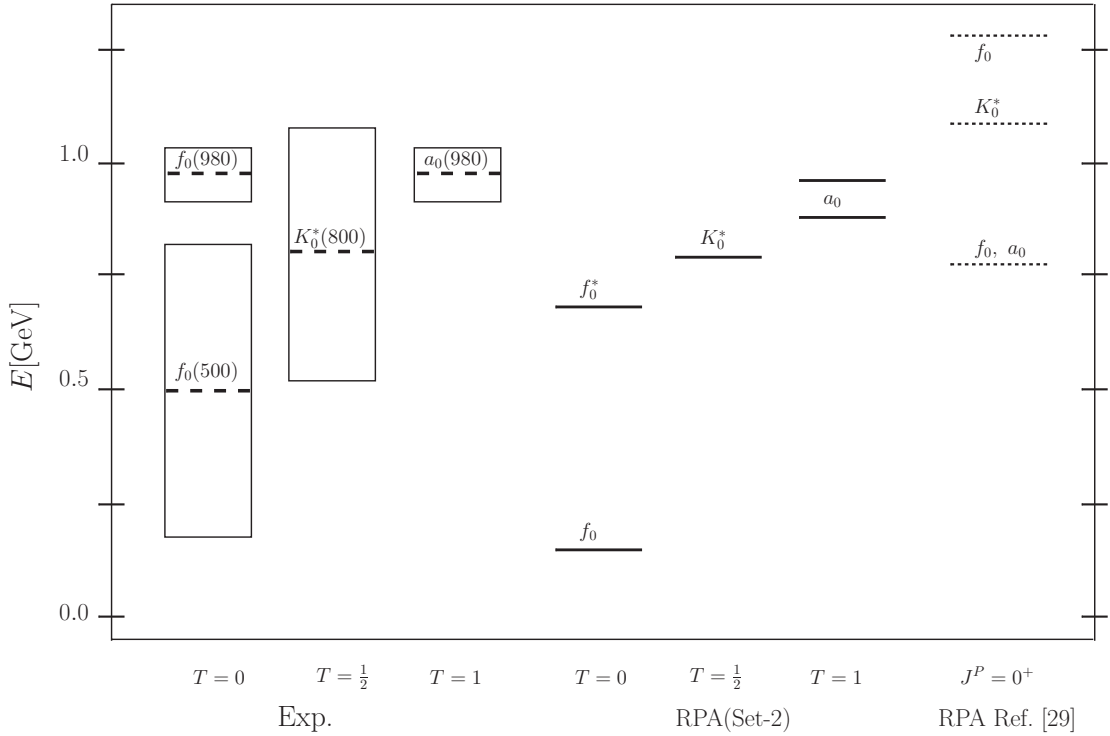


FIG. 2: Results for scalar mesons of Set-2 in the RPA framework, compared with experimental data.

The RPA results for scalar mesons obtained in Table V for Set-2 of Table I, are compared in Figure 2 with the scalar states reported in Ref. [29] and with the experimental values. In our approach, the clearest identification can be made in the sector with  $(Y, T) = (\pm 1, \frac{1}{2})$ , *i.e.*, for the scalar kaon states. For the  $K_0^*(800)$  or  $\kappa$  meson, several experimental data are reported [33]. The theoretical predictions for this state range from 594 MeV to 905 MeV, while the experimental values locate it between 706 and 855 MeV. In our TDA and RPA calculations, we find one state at about 800 MeV. Finally, for the scalar meson with  $(Y, T) = (0, 1)$ , we find two states that fit very well with the  $a_0(980)$ , however, it is hard to say at this time whether the physical  $a_0$  state could correspond to one of these states, or even a mixture of them.

As we have mentioned before, one  $q\bar{q}$  state and one  $s\bar{s}$  state have been used to describe the  $f_0$ - and  $f_0^*$ -like states, respectively. As can be seen from Figure 2, the results obtained in [29] do not show a second  $f_0$  state below 1 GeV,

and their  $f_0$  and  $a_0$  states are degenerate. In our calculations, the  $f_0$ - and  $a_0$ -like states belong to different subspaces. The subspace containing the  $a_0$ -like state does not allow  $s\bar{s}$ -quark representations.

The understanding of the structure of the rather controversial scalar states requires, in addition, the calculation of their widths, something that is beyond the scope of the present work. Such a calculation will also provide some insights about one state that appears in the  $(Y, T) = (\pm 1, \frac{1}{2})$ -sector of the TDA and RPA results at about 480 MeV, and two states in the  $(Y, T) = (0, 1)$ -sector located at about 200 and 550 MeV, respectively. These states could be background states to those reported in Table V, which may lead to a very broad state rather than a sharp one.

### B. Renormalization of the parameters.

In this section we briefly discuss the numerical renormalization of the masses and interaction strengths. As we mentioned in Section II A, in order to maintain the observables unchanged, we need to renormalize the quark masses and the couplings of the Hamiltonian when the cut-off ( $N_{\text{cut}}$ ) of the harmonic oscillator basis is increased. In Appendix E, we explain the philosophy of the renormalization and the ansatz used to renormalize the quark masses and the couplings in more detail.

In Table VI, we show the variation of the masses and interaction parameters with the cut-off that maintains the single-particle energies, ( $\varepsilon_{k,j,Y,T}$  with  $j = \frac{1}{2}$ ) for each flavor-isospin, *i.e.*,  $m_q^{eff} = \varepsilon_{1,\frac{1}{2},\pm\frac{1}{2},\frac{1}{2}}$  and  $m_s^{eff} = \varepsilon_{1,\frac{1}{2},0,0}$ , invariant. As a result, the RPA spectrum also remains approximately invariant.

$N_{\text{cut}}$	$m_q[\text{GeV}]$	$m_s[\text{GeV}]$	$\alpha$	$\beta[\text{GeV}^2]$	$m_q^{eff}[\text{GeV}]$	$m_s^{eff}[\text{GeV}]$	$\pi_{RPA}[\text{GeV}]$
3	0.050	0.310	0.16	0.40	0.258	0.400	0.136
5	0.142	0.337	0.23	0.28	0.258	0.400	0.136
7	0.173	0.351	0.29	0.22	0.258	0.400	0.137
9	0.191	0.360	0.33	0.19	0.258	0.400	0.138
11	0.202	0.367	0.38	0.17	0.258	0.400	0.138
13	0.210	0.371	0.42	0.15	0.258	0.400	0.137

TABLE VI: Numerical renormalization of the masses and interaction parameters.

As an example, we show in Table VI the mass of the RPA pion-like state as a function of the cut-off. The mass of this state remains approximately constant, while the quark masses and the couplings change according to

$$m_{N_{\text{cut}}}^f = m_{N_0}^f \sqrt{x_{N_{\text{cut}}}^f} \quad (19)$$

and

$$\begin{aligned} \alpha_{N_{\text{cut}}} &= \alpha_{N_0} \sqrt{x_{N_{\text{cut}}}} \\ \beta_{N_{\text{cut}}} &= \beta_{N_0} / \sqrt{x_{N_{\text{cut}}}} \end{aligned} \quad (20)$$

with  $x_{N_{\text{cut}}} \approx 1 + t_1 (N_{\text{cut}} - N_0)^{t_2}$  and  $x_{N_{\text{cut}}}^f \approx 1 + t_1^f (N_{\text{cut}} - N_0)^{t_2^f}$ , respectively. The superscript  $f = q, s$  distinguishes between the up, down ( $q = u = d$ ) and strange ( $s$ ) quarks.

In Figure 3, we show the dimensionless values  $\tilde{m}_q = \frac{m_q^{N_{\text{cut}}}}{m_q^{N_0}}$ ,  $\tilde{m}_s = \frac{m_s^{N_{\text{cut}}}}{m_s^{N_0}}$ ,  $\tilde{\alpha} = \frac{\alpha_{N_{\text{cut}}}}{\alpha_{N_0}}$  and  $\tilde{\beta} = \frac{\beta_{N_{\text{cut}}}}{\beta_{N_0}}$  as functions of the cut-off.

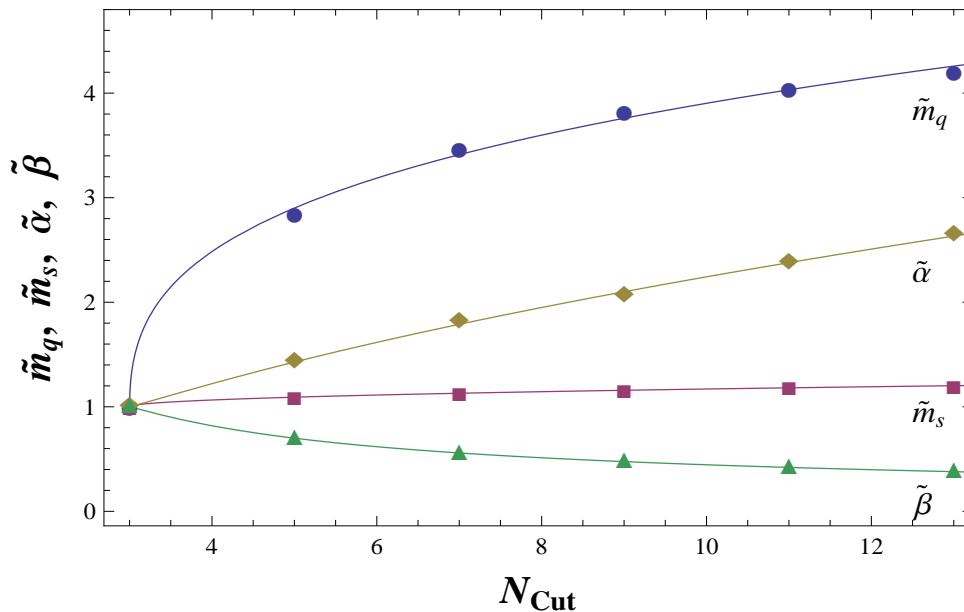


FIG. 3: Renormalization of the masses and interaction constants as a function of  $N_{\text{cut}}$ .

The values for the parameters  $t_1, t_2, t_1^f, t_2^f$  are listed in Table VII.

$t_1$	$t_2$	$t_1^q$	$t_2^q$	$t_1^s$	$t_2^s$
0.49	1.08	5.17	0.52	0.13	0.52

TABLE VII: Numerical fits for the parameters of the renormalization functions in Eqs. (19) and (20).

Based on the results of Table VII, the renormalization of the parameters can be written in the simpler form

$$\begin{aligned}
 m_{N_{\text{cut}}}^f &= m_{N_0}^f \sqrt{1 + t_1^f (N_{\text{cut}} - N_0)^{\frac{1}{2}}} \\
 \alpha_{N_{\text{cut}}} &= \alpha_{N_0} \sqrt{1 + \frac{1}{2} (N_{\text{cut}} - N_0)} \\
 \beta_{N_{\text{cut}}} &= \frac{\beta_{N_0}}{\sqrt{1 + \frac{1}{2} (N_{\text{cut}} - N_0)}} .
 \end{aligned} \tag{21}$$

#### IV. CONCLUSIONS

We have applied standard many-body methods, adapted from the nuclear many-body problem, to a simplified effective QCD Hamiltonian suitable for the description of low-lying mesons. The interaction between color-charge densities was approximated by a combination of a Coulomb plus linear confining potential, which takes the gluon contribution into account in an effective way. We have used the harmonic oscillator wave functions as a basis for the quantization of the fermion fields. It was shown that this basis is quite convenient for the calculations.

A prediagonalization of the kinetic energy term was performed, which provided a basis where effective quarks and antiquarks operators could be defined. We deduced all the expressions for the QCD-motivated Hamiltonian in this effective basis. Then, the Hamiltonian was diagonalized in the basis of quark and antiquark pairs, by means of both the *Tamm-Dancoff Approximation* (TDA) and the *Random Phase Approximation* (RPA). The building blocks in this part of the calculation are effective quarks and antiquarks coupled to color singlets. The meson spectrum below 1 GeV was calculated for configurations belonging to subspaces with quantum numbers  $\{J^P, (Y, T)\}$  of pseudoscalar,



vector and scalar states. In the subspaces with  $(Y, T) = (0, 0)$ , the simplified version of the color confining interaction used in this approach, was not able to generate dynamical flavor mixing.

For the meson-like states we obtain the following results:

- i) The pion-like state of the RPA scheme, when the parameter  $\alpha$  of the interaction is different from zero, is in better agreement with the experimental value than the TDA one, for the same parametrization. This is due to the ground state correlations present in the RPA framework.
- ii) The kaon-like states are well reproduced. These states are not influenced by the ground state correlations due to the scalar structure of the RPA vacuum in the flavor-isospin channel.
- iii) In this description, we were able to accommodate scalar mesons. This may contribute to clarify the controversies found in the literature about these states.
- iv) Besides the  $\eta$ - and  $f_0$ -like states, which in the RPA scheme are quite low with respect to the data, the rest of the light meson spectrum is well reproduced, as shown in Figures 1 and 2. The difficulty with the  $\eta$ - and  $f_0$ -like states is a clear indication of the lack of a dynamical flavor mixing term in the Hamiltonian used here. To incorporate the corresponding virtual pair annihilation processes in our approach would require the introduction of dynamical gluonic degrees of freedom, so that the Hamiltonian could allow for a mixing of quark-antiquark states with states of at least two dynamical gluons.

In the present approach, we have adjusted the parameters by fitting the pion-like state within the RPA scheme to the experimental value. The rest of the spectrum is a consequence of such a fit, because we have not performed further adjustment of the masses and couplings appearing in the model.

The renormalization procedure of the parameters in terms of the cut-off of the configurational space,  $N_{\text{cut}}$ , was presented in Section III B and Appendix E. We have shown that after the renormalization, the RPA results are weakly dependent on the cut-off.

The present work shows that the TDA and RPA many-body methods can give valuable insight into the non-perturbative regime of QCD. The procedure described here provides a straightforward manner to calculate the complete spectrum of hadron states, and it can be extended towards more complete effective descriptions of QCD.

### Acknowledgements

One of the authors (T.Y-M) thanks the National Research Council of Argentina (CONICET) for a post-doctoral scholarships. (O.C.) is a member of the scientific career of the CONICET. (P.O.H and D.A.A-Q) acknowledges financial help from DGAPA-PAPIIT (IN100315) and from CONACYT (Mexico, grant 251817). This work has been supported financially by the CONICET (PIP-282) and by the ANPCYT. D.A.A-Q. acknowledges a scholarship received from CONACyT. A.W. is grateful to the Instituto de Ciencias Nucleares of Universidad Nacional Aut3noma de M3xico for the warm hospitality extended to him during a five-months stay in 2016. He also acknowledges support by Conacyt project no. CB-2013/222812 and by CIC-UMSNH.

### Appendix A: The kinetic energy and the effective basis

The kinetic energy in terms of the creation and annihilation operators in the harmonic oscillator basis is given by [25]

$$\mathbf{K} = \sum_{j\tau_1 N_1 l_1} \sum_{mcf} K_{\tau_1(N_1 l_1), \tau_2(N_2 l_2)}^{j,T} \mathbf{q}_{\tau_1(N_1 l_1)j m c f}^\dagger \mathbf{q}^{\tau_2(N_2 l_2)j m c f} \quad , \quad (\text{A1})$$

where the matrix elements are

$$K_{\tau_1(N_1 l_1), \tau_2(N_2 l_2)}^{j,T} = \begin{cases} k_{N_1 N_2}^j & \text{if } l_1 = j + \frac{1}{2}, l_2 = j - \frac{1}{2}, \tau_1 \neq \tau_2 \\ k_{N_2 N_1}^j & \text{if } l_1 = j - \frac{1}{2}, l_2 = j + \frac{1}{2}, \tau_1 \neq \tau_2 \\ m_0^T & \text{if } (N_1 l_1) = (N_2 l_2), \tau_1 = \tau_2 = +\frac{1}{2} \\ -m_0^T & \text{if } (N_1 l_1) = (N_2 l_2), \tau_1 = \tau_2 = -\frac{1}{2} \\ 0 & \text{in all other cases} \end{cases} \quad , \quad (\text{A2})$$

and  $k_{N N'}^j$  is defined as [25]

$$k_{N N'}^j = \sqrt{B_0} \left( \sqrt{\frac{N - j + \frac{3}{2}}{2}} \delta_{N', N+1} + \sqrt{\frac{N + j + \frac{3}{2}}{2}} \delta_{N', N-1} \right) \quad . \quad (\text{A3})$$

The diagonalization of the kinetic energy implies a transformation to a new basis of creation operators

$$\mathbf{q}_{\tau(Nl)jmcf}^{\dagger} = \sum_{\lambda\pi k} \left( \alpha_{\tau(Nl),\lambda\pi k}^{j,T} \right)^* \mathbf{Q}_{\lambda\pi k j m c f}^{\dagger} \delta_{\pi,(-1)^{\frac{1}{2}-\tau+l}} \quad , \quad (\text{A4})$$

where we may take the transformation coefficients  $\alpha_{\tau(Nl),\lambda\pi k}^{j,T}$  to be real.

After the prediagonalization in Eq. (6), the association with quarks and antiquarks is, according to the Dirac picture,

$$\begin{aligned} \mathbf{Q}_{\frac{1}{2}\pi k j m c f}^{\dagger} &\rightarrow \mathbf{b}_{\pi k j m c f}^{\dagger} \\ \mathbf{Q}_{-\frac{1}{2}\pi k j m c f}^{\dagger} &\rightarrow \mathbf{d}_{\pi k j m c f} \quad . \end{aligned} \quad (\text{A5})$$

The operator  $\mathbf{b}_{\pi k j m c f}^{\dagger}$  is a quark creation operator and  $\mathbf{d}_{\pi k j m c f}$  an antiquark annihilation operator with lower indices.

The rule to raise and lower indices is taken from [41],

$$\begin{aligned} \mathbf{b}^{\dagger\pi k j m \bar{c} \bar{f}} &= (-1)^{\chi_f} (-1)^{\chi_c+j+m} \mathbf{b}_{\pi k j - m c f}^{\dagger} \\ \mathbf{b}_{\pi k j m c f}^{\dagger} &= (-1)^{\chi_f} (-1)^{\chi_c+j-m} \mathbf{b}^{\dagger\pi k j - m \bar{c} \bar{f}} \\ \mathbf{b}^{\pi k j m c f} &= (-1)^{\chi_f} (-1)^{\chi_c+j-m} \mathbf{b}_{\pi k j - m \bar{c} \bar{f}} \\ \mathbf{b}_{\pi k j m \bar{c} \bar{f}} &= (-1)^{\chi_f} (-1)^{\chi_c+j+m} \mathbf{b}^{\pi k j - m c f} \quad , \end{aligned} \quad (\text{A6})$$

and similarly,

$$\begin{aligned} \mathbf{d}^{\dagger\pi k j m c f} &= (-1)^{\chi_f} (-1)^{\chi_c+j+m} \mathbf{d}_{\pi k j - m \bar{c} \bar{f}}^{\dagger} \\ \mathbf{d}_{\pi k j m \bar{c} \bar{f}}^{\dagger} &= (-1)^{\chi_f} (-1)^{\chi_c+j-m} \mathbf{d}^{\dagger\pi k j - m c f} \\ \mathbf{d}^{\pi k j m \bar{c} \bar{f}} &= (-1)^{\chi_f} (-1)^{\chi_c+j-m} \mathbf{d}_{\pi k j - m c f} \\ \mathbf{d}_{\pi k j m c f} &= (-1)^{\chi_f} (-1)^{\chi_c+j+m} \mathbf{d}^{\pi k j - m \bar{c} \bar{f}} \quad . \end{aligned} \quad (\text{A7})$$

The phase  $(-1)^{\chi_f}$  is a short hand notation for  $(-1)^{\frac{1}{3}+\frac{Y}{2}+T_z}$  [31]. The equivalent notation holds for the color part.

Since we require a unitary transformation which conserves the anti-commutation relations  $\left\{ \mathbf{Q}_{\lambda_1\pi_1 k_1 j_1 \mu_1}^{\dagger}, \mathbf{Q}_{\lambda_2\pi_2 k_2 j_2 \mu_2}^{\dagger} \right\} = \delta_{\lambda_2\lambda_1} \delta_{\pi_2\pi_1} \delta_{j_2 j_1} \delta_{k_2 k_1} \delta_{\mu_2 \mu_1}$  with  $\mu_i = m_i c_i f_i$ , we have

$$\begin{aligned} \left\{ \mathbf{q}_{\tau_1(N_1 l_1) j m_1 c_1 f_1}^{\dagger}, \mathbf{q}_{\tau_2(N_2 l_2) j m_2 c_2 f_2}^{\dagger} \right\} &= \delta_{\tau_2 \tau_1} \delta_{N_2 N_1} \delta_{l_2 l_1} \delta_{m_2 m_1} \delta_{c_2 c_1} \delta_{f_2 f_1} \\ &= \sum_{\lambda\pi k} \alpha_{\tau_1(N_1 l_1),\lambda\pi k}^{j,T_1} \alpha_{\tau_2(N_2 l_2),\lambda\pi k}^{j,T_2} \delta_{m_2 m_1} \delta_{c_2 c_1} \delta_{f_2 f_1} \quad , \end{aligned} \quad (\text{A8})$$

where  $\delta_{f_2 f_1}$  is a short notation for  $\delta_{Y_2 Y_1} \delta_{T_2 T_1} \delta_{T_{2z} T_{1z}}$ . Thus the matrix  $\alpha$  is unitary and satisfies the orthogonality relation

$$\sum_{\lambda\pi k} \alpha_{\tau_1(N_1 l_1),\lambda\pi k}^{j,T} \alpha_{\tau_2(N_2 l_2),\lambda\pi k}^{j,T} = \delta_{\tau_2 \tau_1} \delta_{N_2 N_1} \delta_{l_2 l_1} \quad . \quad (\text{A9})$$

## Appendix B: The Coulomb-Hamiltonian

The Coulomb Hamiltonian in (2) is written in terms of the fermion creation and annihilation operators of Eq. (3). The SU(3) color generators  $T_C$  and  $T^C$  in Eq. (2) are rewritten in terms of SU(3) Clebsch-Gordan coefficients [31]. Starting from  $(T_C)_{c_2}^{c_1} = \langle (1,0)c_1 | T_C | (1,0)c_2 \rangle$  and applying the Wigner Eckart Theorem, we obtain

$$(T_C)_{c_2}^{c_1} = (-1)^{\chi_{c_2}+1} \frac{1}{\sqrt{2}} \langle (1,0)c_1, (0,1)\bar{c}_2 | (1,1)C \rangle_1 \quad . \quad (\text{B1})$$

The Coulomb Hamiltonian then takes the form

$$\begin{aligned}
\mathbf{H}_{\text{Coul}} &= -\frac{1}{2} \sum_C \sum_{\tau_i N_i l_i m_i j_i m_i \sigma_i f_i c_i} (-1)^{X_C} \delta_{\tau_1 \tau_2} \delta_{\tau_3 \tau_4} \delta_{\sigma_1 \sigma_2} \delta_{\sigma_3 \sigma_4} \delta_{f_1 f_2} \delta_{f_3 f_4} \\
&\times \left[ \langle l_1 m_{l_1}, \frac{1}{2} \sigma_1 \mid j_1 m_1 \rangle \langle l_2 m_{l_2}, \frac{1}{2} \sigma_2 \mid j_2 m_2 \rangle \frac{(-1)^{X_{c_2}+1}}{\sqrt{2}} \langle (10)c_1, (01)\bar{c}_2 \mid (11)C \rangle_1 \mathbf{q}_{\tau_1(N_1 l_1) j_1 m_1 c_1 f_1}^{\dagger} \mathbf{q}^{\tau_2(N_2 l_2) j_2 m_2 c_2 f_2} \right] \\
&\times \left[ \langle l_3 m_{l_3}, \frac{1}{2} \sigma_3 \mid j_3 m_3 \rangle \langle l_4 m_{l_4}, \frac{1}{2} \sigma_4 \mid j_4 m_4 \rangle \frac{(-1)^{X_{c_4}+1}}{\sqrt{2}} \langle (10)c_3, (01)\bar{c}_4 \mid (11)\bar{C} \rangle_1 \mathbf{q}_{\tau_3(N_3 l_3) j_3 m_3 c_3 f_3}^{\dagger} \mathbf{q}^{\tau_4(N_4 l_4) j_4 m_4 c_4 f_4} \right] \\
&\times \int d\mathbf{x} d\mathbf{y} \Psi_{N_1 l_1 m_{l_1}}^*(\mathbf{x}) \Psi_{N_2 l_2 m_{l_2}}(\mathbf{x}) V(|\mathbf{x} - \mathbf{y}|) \Psi_{N_3 l_3 m_{l_3}}^*(\mathbf{y}) \Psi_{N_4 l_4 m_{l_4}}(\mathbf{y}) \quad , \quad (\text{B2})
\end{aligned}$$

where  $\Psi_{N l m_i}(\mathbf{x})$  are the three-dimensional harmonic oscillator wave functions. In Eq. (B2), the presence of  $\delta_{\tau_1 \tau_2} \delta_{\tau_3 \tau_4}$ ,  $\delta_{\sigma_1 \sigma_2} \delta_{\sigma_3 \sigma_4}$  and  $\delta_{f_1 f_2} \delta_{f_3 f_4}$  arises from the color charge-density structure which does not contain any pseudospin, spin or flavor-isospin dependence.

Let us concentrate for a moment on the integral over  $\mathbf{x}$  and  $\mathbf{y}$ . By recoupling we obtain

$$\begin{aligned}
&\sum_{J' M'_J J M_J} \langle l_1 m_{l_1}, l_3 m_{l_3} \mid J' M'_J \rangle \langle l_2 m_{l_2}, l_4 m_{l_4} \mid J M_J \rangle \\
&\times \int d\mathbf{x} d\mathbf{y} [\Psi_{N_1 l_1}^*(\mathbf{x}) \otimes \Psi_{N_3 l_3}^*(\mathbf{y})]_{M'_J}^{J'} V(|\mathbf{x} - \mathbf{y}|) [\Psi_{N_2 l_2}(\mathbf{x}) \otimes \Psi_{N_4 l_4}(\mathbf{y})]_{M_J}^J \quad . \quad (\text{B3})
\end{aligned}$$

Using the Moshinsky brackets (round brackets) [42, 43] for recoupling the integral in Eq. (B3), we get

$$\begin{aligned}
&\sum_{N'_r l'_r, N_r l_r; N'_R L'_R, N_R L_R} (N'_r l'_r, N'_R L'_R, J' \mid N_1 l_1, N_3 l_3, J') (N_r l_r, N_R L_R, J \mid N_2 l_2, N_4 l_4, J) \\
&\times \int d\mathbf{r} d\mathbf{R} [\Psi_{N'_R L'_R}^*(\mathbf{R}) \otimes \Psi_{N'_r l'_r}^*(\mathbf{r})]_{M'_J}^{J'} V(\sqrt{2}r) [\Psi_{N_R L_R}(\mathbf{R}) \otimes \Psi_{N_r l_r}(\mathbf{r})]_{M_J}^J \quad , \quad (\text{B4})
\end{aligned}$$

where  $\mathbf{R} = \frac{1}{\sqrt{2}}(\mathbf{x} + \mathbf{y})$  refers to the *Center of Mass* (CM) and  $\mathbf{r} = \frac{1}{\sqrt{2}}(\mathbf{x} - \mathbf{y})$  to the relative coordinate. Since in the last equation the potential is  $R$ -independent, we can easily integrate over  $R$ . Then the integral in Eq. (B4) becomes

$$\begin{aligned}
&\sum_{M'_R M_R; m'_r m_r} \langle L'_R M'_R, l'_r m'_r \mid J' M'_J \rangle \langle L_R M_R, l_r m_r \mid J M_J \rangle \\
&\int d\mathbf{R} \Psi_{N'_R L'_R M'_R}^*(\mathbf{R}) \Psi_{N_R L_R M_R}(\mathbf{R}) \int d\mathbf{r} \Psi_{N'_r l'_r m'_r}^*(\mathbf{r}) V(\sqrt{2}r) \Psi_{N_r l_r m_r}(\mathbf{r}) \\
&= \delta_{N'_R N_R} \delta_{L'_R L_R} \sum_{M_R; m'_r m_r} \langle L_R M_R, l'_r m'_r \mid J' M'_J \rangle \langle L_R M_R, l_r m_r \mid J M_J \rangle \int d\mathbf{r} \Psi_{N'_r l'_r m'_r}^*(\mathbf{r}) V(\sqrt{2}r) \Psi_{N_r l_r m_r}(\mathbf{r}) \quad . \quad (\text{B5})
\end{aligned}$$

Since  $V$  is a scalar, we have as an additional constraint that  $l'_r = l_r$  and  $m'_r = m_r$ . The integral itself does not depend on  $m_r$ , thus we can replace  $m_r$  by  $l_r$ . With this replacement, the summation over  $M_R, m'_r, m_r$  with the two Clebsch-Gordan coefficients becomes a summation over  $M_R, m_r$  and represents the orthogonality relation of the Clebsch-Gordan coefficients, thus leading to  $\delta_{J' J} \delta_{M'_J M_J}$ .

With all this, equation (B3) takes the form

$$\begin{aligned}
&\sum_{J M_J; N'_r N_r l_r; N_R L_R} \langle l_1 m_{l_1}, l_3 m_{l_3} \mid J M_J \rangle \langle l_2 m_{l_2}, l_4 m_{l_4} \mid J M_J \rangle \\
&\times (N'_r l_r, N_R L_R, J \mid N_1 l_1, N_3 l_3, J) (N_r l_r, N_R L_R, J \mid N_2 l_2, N_4 l_4, J) \int d\mathbf{r} \Psi_{N'_r l_r l_r}^*(\mathbf{r}) V(\sqrt{2}r) \Psi_{N_r l_r l_r}(\mathbf{r}) \quad . \quad (\text{B6})
\end{aligned}$$

Using (B6), the Hamiltonian (B2) can be written

$$\begin{aligned}
\mathbf{H}_{\text{Coul}} = & -\frac{1}{2} \sum_{N_i l_i m_i, j_i m_i, \sigma_i} \sum_{JM_J N_r' l_r N_R L_R} \delta_{\sigma_1 \sigma_2} \delta_{\sigma_3 \sigma_4} \frac{1}{2} \langle l_1 m_{l_1}, \frac{1}{2} \sigma_1 | j_1 m_1 \rangle \langle l_2 m_{l_2}, \frac{1}{2} \sigma_1 | j_2 m_2 \rangle \\
& \times \langle l_3 m_{l_3}, \frac{1}{2} \sigma_3 | j_3 m_3 \rangle \langle l_4 m_{l_4}, \frac{1}{2} \sigma_3 | j_4 m_4 \rangle \langle l_1 m_{l_1}, l_3 m_{l_3} | JM_J \rangle \langle l_2 m_{l_2}, l_4 m_{l_4} | JM_J \rangle \\
& \times (N_r' l_r, N_R L_R, J | N_1 l_1, N_3 l_3, J) (N_r l_r, N_R L_R, J | N_2 l_2, N_4 l_4, J) \int d\mathbf{r} \Psi_{N_r' l_r l_r}^*(\mathbf{r}) V(\sqrt{2}r) \Psi_{N_r l_r l_r}(\mathbf{r}) \\
& \times \left\{ \sum_C (-1)^{\chi_C} \sum_{c_i \tau_i f_i} \delta_{\tau_1 \tau_2} \delta_{\tau_3 \tau_4} \delta_{f_1 f_2} \delta_{f_3 f_4} \langle (10)c_1, (01)\bar{c}_2 | (11)C \rangle_1 \langle (10)c_3, (01)\bar{c}_4 | (11)\bar{C} \rangle_1 (-1)^{\frac{1}{2} - \tau_2 + \frac{1}{2} - \tau_4} \right. \\
& \left. \times (-1)^{j_2 - m_2 + j_4 - m_4} (-1)^{\chi_{f_2} + \chi_{f_4}} \mathbf{q}_{\tau_1(N_1 l_1) j_1 m_1 c_1 f_1}^\dagger \mathbf{q}_{-\tau_2(N_2 l_2) j_2 - m_2 \bar{c}_2 \bar{f}_2} \mathbf{q}_{\tau_3(N_3 l_3) j_3 m_3 c_3 f_3}^\dagger \mathbf{q}_{-\tau_4(N_4 l_4) j_4 - m_4 \bar{c}_4 \bar{f}_4} \right\}. \tag{B7}
\end{aligned}$$

The phase  $(-1)^{\chi_{c_2} + \chi_{c_4}}$  appearing in Eq. (B2) is canceled in Eq. (B7) against the same phase resulting from lowering the indices of the operators. The remaining  $(-1)^{\chi_C}$  phase is proportional to the SU(3) coupling to color zero, where the factor  $1/\sqrt{8}$  is missing. The contraction over  $\tau_i$  (*i.e.*,  $(-1)^{\frac{1}{2} - \tau_2} \delta_{\tau_1 \tau_2}$ ) and  $f_i$  (*i.e.*,  $(-1)^{\chi_{f_2}} \delta_{f_1 f_2}$ ) also represents a coupling to zero, without the factor  $1/\sqrt{2}$  in the first case and the factor  $1/\sqrt{3}$  in the second case. Correcting for these factors, we have for the expression  $\{\dots\}$  in Eq. (B7),

$$\begin{aligned}
\left\{ \dots \right\} = & \sum_{LM_L} (-1)^{j_2 - m_2 + j_4 - m_4} (\sqrt{2})^2 (\sqrt{3})^2 \sqrt{8} \langle j_1 m_1, j_2 - m_2 | LM_L \rangle \langle j_3 m_3, j_4 - m_4 | L - M_L \rangle \frac{(-1)^{L - M_L}}{\sqrt{2L + 1}} \\
& \times \left[ \left[ \mathbf{q}_{(N_1 l_1) j_1}^\dagger \otimes \mathbf{q}_{(N_2 l_2) j_2} \right]^{0L(11)(00)} \otimes \left[ \mathbf{q}_{(N_3 l_3) j_3}^\dagger \otimes \mathbf{q}_{(N_4 l_4) j_4} \right]^{0L(11)(00)} \right]_{00 \ 0 \ 0}^{00(00)(00)}. \tag{B8}
\end{aligned}$$

The intermediate and total couplings are ordered in the following way: pseudo-spin, angular momentum, color and flavor.

As a result, we can rewrite the Coulomb Hamiltonian (Eq. (B2)) as

$$\begin{aligned}
\mathbf{H}_{\text{Coul}} = & -\frac{1}{2} \sum_{N_i l_i m_i, j_i m_i, \sigma_i, LM_L} \sum_{JM_J N_r' l_r N_R L_R} \frac{1}{2} (\sqrt{2})^2 (\sqrt{3})^2 \sqrt{8} (-1)^{j_2 - m_2 + j_4 - m_4} \frac{(-1)^{L - M_L}}{\sqrt{2L + 1}} \\
& \times \langle l_1 m_{l_1}, \frac{1}{2} \sigma_1 | j_1 m_1 \rangle \langle l_2 m_{l_2}, \frac{1}{2} \sigma_1 | j_2 m_2 \rangle \langle j_1 m_1, j_2 - m_2 | LM_L \rangle \\
& \times \langle l_3 m_{l_3}, \frac{1}{2} \sigma_3 | j_3 m_3 \rangle \langle l_4 m_{l_4}, \frac{1}{2} \sigma_3 | j_4 m_4 \rangle \langle j_3 m_3, j_4 - m_4 | L - M_L \rangle \\
& \times \langle l_1 m_{l_1}, l_3 m_{l_3} | JM_J \rangle \langle l_2 m_{l_2}, l_4 m_{l_4} | JM_J \rangle \\
& \times (N_r' l_r, N_R L_R, J | N_1 l_1, N_3 l_3, J) (N_r l_r, N_R L_R, J | N_2 l_2, N_4 l_4, J) \int d\mathbf{r} \Psi_{N_r' l_r l_r}^*(\mathbf{r}) V(\sqrt{2}r) \Psi_{N_r l_r l_r}(\mathbf{r}) \\
& \times \left[ \left[ \mathbf{q}_{(N_1 l_1) j_1}^\dagger \otimes \mathbf{q}_{(N_2 l_2) j_2} \right]^{0L(11)(00)} \otimes \left[ \mathbf{q}_{(N_3 l_3) j_3}^\dagger \otimes \mathbf{q}_{(N_4 l_4) j_4} \right]^{0L(11)(00)} \right]_{00 \ 0 \ 0}^{00(00)(00)}. \tag{B9}
\end{aligned}$$

Using the well-known relations for the sums of the products of three and four Clebsch-Gordan coefficients [44], we arrive at the final expression for the Coulomb interaction,

$$\mathbf{H}_{\text{Coul}} = -\frac{1}{2} \sum_{N_i l_i j_i L} V_{\{N_i l_i j_i\}}^L \left[ \left[ \mathbf{q}_{(N_1 l_1) j_1}^\dagger \otimes \mathbf{q}_{(N_2 l_2) j_2} \right]^{0L(11)(00)} \otimes \left[ \mathbf{q}_{(N_3 l_3) j_3}^\dagger \otimes \mathbf{q}_{(N_4 l_4) j_4} \right]^{0L(11)(00)} \right]_{00 \ 0 \ 0}^{00(00)(00)}, \tag{B10}$$

with

$$\begin{aligned}
V_{\{N_i l_i j_i\}}^L &= \sum_{J N_r' N_r N_R L_R} 3\sqrt{8}\sqrt{(2j_1+1)(2j_2+1)(2j_3+1)(2j_4+1)}\sqrt{2L+1}(2J+1) \\
&\times (-1)^{L+j_2+j_4-J+1} \begin{Bmatrix} l_1 & L & l_2 \\ j_2 & \frac{1}{2} & j_1 \end{Bmatrix} \begin{Bmatrix} l_3 & L & l_4 \\ j_4 & \frac{1}{2} & j_3 \end{Bmatrix} \begin{Bmatrix} l_2 & J & l_4 \\ l_3 & L & l_1 \end{Bmatrix} \\
&\times (N_r' l_r, N_R L_R, J | N_1 l_1, N_3 l_3, J)(N_r l_r, N_R L_R, J | N_2 l_2, N_4 l_4, J) \int d^3 r \Psi_{N_r' l_r l_r}^*(\vec{r}) V(\sqrt{2}r) \Psi_{N_r l_r l_r}(\vec{r}) .
\end{aligned} \tag{B11}$$

The integral over  $r$  in Eq. (B11) is a standard one for the three-dimensional harmonic oscillator. Note that this is an *analytic expression* which is easy to compute.

### Appendix C: The TDA and RPA methods.

The RPA method can be seen as a direct extension of the TDA method where the collective  $ph$ -operator is written (using the notation of Eq. (14)) as

$$\hat{\Gamma}_{n;\Gamma\mu}^\dagger = \sum_{\mathbf{a},\mathbf{b}} X_{\mathbf{ab};\Gamma}^n [\mathbf{b}_\mathbf{a}^\dagger \mathbf{d}_\mathbf{b}^\dagger]_\mu^\Gamma , \tag{C1}$$

which restricts the approximation to the space of  $1p - 1h$  excitations, relevant for low-lying states. The  $n$ th TDA excited state is given by  $|n; \Gamma\mu\rangle = \hat{\Gamma}_{n;\Gamma\mu}^\dagger |\tilde{0}\rangle$ , and the ground state satisfies  $\hat{\Gamma}^{n;\Gamma\mu} |\tilde{0}\rangle = 0$ .

The TDA equation of motion is

$$\sum_{\mathbf{a},\mathbf{b}} \langle \tilde{0} | \left[ \left( [\mathbf{b}_\mathbf{a}'^\dagger \mathbf{d}_\mathbf{b}'^\dagger]_{\mu'}^{\Gamma'} \right)^\dagger, \left[ \mathbf{H}^{QCD}, [\mathbf{b}_\mathbf{a}^\dagger \mathbf{d}_\mathbf{b}^\dagger]_\mu^\Gamma \right] \right] | \tilde{0} \rangle X_{\mathbf{ab};\Gamma}^n = E_{n;\Gamma'}^{TD A} X_{\mathbf{a}'\mathbf{b}';\Gamma'}^n \delta_{\Gamma'\Gamma} \delta_{\mu'\mu} , \tag{C2}$$

where the  $1p - 1h$  correlations are taken into account in the excited states, keeping the ground state  $|\tilde{0}\rangle$  unchanged, and

$$\begin{aligned}
& \left( [\mathbf{b}_\mathbf{a}^\dagger \mathbf{d}_\mathbf{b}^\dagger]_\mu^\Gamma \right)^\dagger \\
&= \left( [\mathbf{b}_{\pi_a k_a j_a Y_a T_a}^\dagger \otimes \mathbf{d}_{\pi_b k_b j_b \bar{Y}_b T_b}^\dagger ]_{M_J, 0, T_z}^{J^P, (0,0), YT} \right)^\dagger \\
&= \sum_{m_a, c_a, T_{az}} \sum_{m_b, c_b, T_{bz}} \langle j_a m_a, j_b - m_b | JM_J \rangle \langle (10)c_a, (01)\bar{c}_b | (0,0)0 \rangle_1 \langle T_a T_{az}, T_b - T_{bz} | TT_z \rangle \\
&\times \mathbf{d}^{\pi_b k_b j_b - m_b, \bar{c}_b \bar{Y}_b, T_b - T_{bz}} \mathbf{b}^{\pi_a k_a j_a m_a, c_a, Y_a, T_a T_{az}} \\
&= \langle \mathbf{a}\mu_\mathbf{a}, \bar{\mathbf{b}}\bar{\mu}_\mathbf{b} | \Gamma\mu \rangle \mathbf{d}^{\bar{\mathbf{b}}\bar{\mu}_\mathbf{b}} \mathbf{b}^{\mathbf{a}\mu_\mathbf{a}} = [\mathbf{d}^{\bar{\mathbf{b}}\bar{\mathbf{b}}\mathbf{a}}]_\mu^\Gamma ,
\end{aligned} \tag{C3}$$

where we have used the short-hand notation  $\langle \mathbf{a}\mu_\mathbf{a}, \bar{\mathbf{b}}\bar{\mu}_\mathbf{b} | \Gamma\mu \rangle$  for the product of the spin, color and isospin-flavor Clebsch-Gordan coefficients. Notice that, whenever the coupling involves upper single-particle indices, we use the Clebsch-Gordan coefficients in the inverted order. This is done for convenience, in order to absorb phases.

The most straightforward generalization of the collective  $1p - 1h$ -operator is the RPA. The phonon creation and annihilation operators are defined as

$$\hat{\Gamma}_{n;\Gamma\mu}^\dagger = \sum_{\mathbf{a},\mathbf{b}} \left\{ X_{\mathbf{ab};\Gamma}^n [\mathbf{b}_\mathbf{a}^\dagger \mathbf{d}_\mathbf{b}^\dagger]_\mu^\Gamma - Y_{\mathbf{ab};\Gamma}^n (-1)^{\phi_{\Gamma\mu}} [\mathbf{d}^{\bar{\mathbf{b}}\bar{\mathbf{b}}\mathbf{a}}]_\mu^{\bar{\Gamma}} \right\} \tag{C4}$$

and

$$\hat{\Gamma}^{n;\Gamma\mu} = \sum_{\mathbf{a},\mathbf{b}} \left\{ (X_{\mathbf{ab};\Gamma}^n)^* [\mathbf{d}^{\bar{\mathbf{b}}\bar{\mathbf{b}}\mathbf{a}}]_\mu^\Gamma - (Y_{\mathbf{ab};\Gamma}^n)^* (-1)^{\phi_{\Gamma\mu}} [\mathbf{b}_\mathbf{a}^\dagger \mathbf{d}_\mathbf{b}^\dagger]_\mu^{\bar{\Gamma}} \right\} , \tag{C5}$$



respectively. The  $n$ th RPA state with quantum numbers  $\Gamma\mu$  is constructed as  $|n; \Gamma\mu\rangle_{RPA} = \hat{\Gamma}_{n; \Gamma\mu}^\dagger |RPA\rangle$ . The RPA ground state  $|RPA\rangle$  is constructed in such a way that the condition  $\hat{\Gamma}^{n; \Gamma\mu} |RPA\rangle = 0$  is fulfilled, *i.e.*,

$$\begin{aligned}
& |RPA\rangle \\
&= |\tilde{0}\rangle + \sum_{n, \Gamma} \sum_{\mathbf{a}'\mathbf{b}'\mathbf{ab}} Z_{\mathbf{a}'\mathbf{b}'\mathbf{ab}}^{n, \Gamma} \left[ [\mathbf{b}_{\mathbf{a}'}^\dagger \mathbf{d}_{\mathbf{b}'}^\dagger]^\Gamma \otimes [\mathbf{b}_{\mathbf{a}}^\dagger \mathbf{d}_{\mathbf{b}}^\dagger]^\Gamma \right]_{0, 0, 0}^{0, (0,0), 00} |\tilde{0}\rangle \\
&= |\tilde{0}\rangle + \sum_{n, \Gamma} \sum_{\mathbf{a}'\mathbf{b}'\mathbf{ab}} Z_{\mathbf{a}'\mathbf{b}'\mathbf{ab}}^{n, \Gamma} \sum_{\mu} \frac{(-1)^{\phi_{\Gamma\mu}}}{\sqrt{\dim(\Gamma)}} [\mathbf{b}_{\mathbf{a}'}^\dagger \mathbf{d}_{\mathbf{b}'}^\dagger]_{\mu}^\Gamma [\mathbf{b}_{\mathbf{a}}^\dagger \mathbf{d}_{\mathbf{b}}^\dagger]_{\bar{\mu}}^\Gamma |\tilde{0}\rangle \\
&= |\tilde{0}\rangle + \sum_{n, \Gamma} \sum_{\mathbf{a}'\mathbf{b}'\mathbf{ab}} Z_{\mathbf{a}'\mathbf{b}'\mathbf{ab}}^{n, \Gamma} \sum_{M_J T_z} \frac{(-1)^{J-M_J}}{\sqrt{2J+1}} \frac{(-1)^{T-T_z}}{\sqrt{2T+1}} \\
&\quad \times [\mathbf{b}_{\pi_{\mathbf{a}'} k_{\mathbf{a}'} j_{\mathbf{a}'} Y_{\mathbf{a}' T_{\mathbf{a}'}}}^\dagger \otimes \mathbf{d}_{\pi_{\mathbf{b}'} k_{\mathbf{b}'} j_{\mathbf{b}'} \bar{Y}_{\mathbf{b}' T_{\mathbf{b}'}}}^\dagger]_{M_J, 0, T_z}^{J^P, (0,0), Y, T} [\mathbf{b}_{\pi_{\mathbf{a}} k_{\mathbf{a}} j_{\mathbf{a}} Y_{\mathbf{a} T_{\mathbf{a}}}}^\dagger \otimes \mathbf{d}_{\pi_{\mathbf{b}} k_{\mathbf{b}} j_{\mathbf{b}} \bar{Y}_{\mathbf{b} T_{\mathbf{b}}}}^\dagger]_{-M_J, 0, -T_z}^{J^P, (0,0), \bar{Y}, T} |\tilde{0}\rangle, \quad (C6)
\end{aligned}$$

with  $\sqrt{\dim(\Gamma)} = \sqrt{2J+1}\sqrt{2T+1}$ ,  $(-1)^{\phi_{\Gamma\mu}} = (-1)^{J-M_J}(-1)^{T-T_z}$  and  $Z_{\mathbf{a}'\mathbf{b}'\mathbf{ab}}^{n, \Gamma} = \sqrt{\dim(\Gamma)} Y_{\mathbf{a}'\mathbf{b}'; \Gamma}^n (X_{\mathbf{ab}; \Gamma}^n)^{-1}$ .

The equation of motion ( $\mathbf{H}^{QCD} |n, \Gamma\mu\rangle = E_{n, \Gamma}^{RPA} |n, \Gamma\mu\rangle$ ) in the RPA formalism is equivalent to the double commutator

$$\langle RPA | \left[ \hat{\Gamma}^{n'; \Gamma\mu}, \left[ \mathbf{H}^{QCD}, \Gamma_{n; \Gamma\mu}^\dagger \right] \right] | RPA \rangle = E_{n; \Gamma}^{RPA} \delta_{n, n'}, \quad (C7)$$

with eigenvalues  $E_{n, \Gamma}^{RPA}$ . Therefore, from Eq. (C7) we get two sets of equations which in matrix form can be written

$$\begin{pmatrix} A & B \\ B^* & A^* \end{pmatrix} \begin{pmatrix} X^n \\ Y^n \end{pmatrix} = E_n^{RPA} \begin{pmatrix} 1 & 0 \\ 0 & -1 \end{pmatrix} \begin{pmatrix} X^n \\ Y^n \end{pmatrix}, \quad (C8)$$

with

$$\begin{aligned}
A_{\mathbf{a}'\mathbf{b}'; \Gamma'\mu'; a, b; \Gamma\mu} &= \langle \tilde{0} | \left[ [\mathbf{d}^{\bar{\mathbf{b}}'} \mathbf{b}^{\mathbf{a}'}]_{\mu'}^{\Gamma'}, \left[ \mathbf{H}^{QCD}, [\mathbf{b}_{\mathbf{a}}^\dagger \mathbf{d}_{\mathbf{b}}^\dagger]_{\mu}^\Gamma \right] \right] | \tilde{0} \rangle, \\
B_{\mathbf{a}'\mathbf{b}'; \Gamma'\mu'; a, b; \Gamma\mu} &= -\langle \tilde{0} | \left[ [\mathbf{d}^{\bar{\mathbf{b}}'} \mathbf{b}^{\mathbf{a}'}]_{\mu'}^{\Gamma'}, \left[ \mathbf{H}^{QCD}, (-1)^{\phi_{\Gamma\mu}} [\mathbf{d}^{\bar{\mathbf{b}}} \mathbf{b}^{\mathbf{a}}]_{\bar{\mu}}^\Gamma \right] \right] | \tilde{0} \rangle
\end{aligned} \quad (C9)$$

being the forward and backward matrices of the RPA method, respectively. They are given explicitly in Appendix D.

To calculate the commutators in Eq. (C9) we enforce the *quasi-boson* approximation

$$\langle RPA | \left[ [\mathbf{d}^{\bar{\mathbf{b}}'} \mathbf{b}^{\mathbf{a}'}]_{\mu'}^{\Gamma'}, [\mathbf{b}_{\mathbf{a}}^\dagger \mathbf{d}_{\mathbf{b}}^\dagger]_{\mu}^\Gamma \right] | RPA \rangle \simeq \langle \tilde{0} | \left[ [\mathbf{d}^{\bar{\mathbf{b}}'} \mathbf{b}^{\mathbf{a}'}]_{\mu'}^{\Gamma'}, [\mathbf{b}_{\mathbf{a}}^\dagger \mathbf{d}_{\mathbf{b}}^\dagger]_{\mu}^\Gamma \right] | \tilde{0} \rangle = \delta_{\mathbf{b}'\mathbf{b}} \delta_{\mathbf{a}'\mathbf{a}} \delta_{\Gamma'\Gamma} \delta_{\mu'\mu}. \quad (C10)$$

**Appendix D: The Forward and Backward matrices of the Effective QCD Hamiltonian.**

The forward matrix elements are given by

$$\begin{aligned}
& A_{a'b';\Gamma'\mu'; a,b;\Gamma\mu} \\
&= \delta_{\Gamma\Gamma'} \delta_{\mu\mu'} \sum_{kj\pi Y T} \epsilon_{kj\pi Y T} \\
&\times \delta_{\pi_a'\pi_a} \delta_{\pi_b'\pi_b} \delta_{k_a'k_a} \delta_{k_b'k_b} \delta_{j_a'j_a} \delta_{j_b'j_b} \delta_{Y_{f_a'}Y_{f_a}} \delta_{Y_{f_b'}Y_{f_b}} \delta_{T_{f_a'}T_{f_a}} \delta_{T_{f_b'}T_{f_b}} (\delta_{k_k a} \delta_{j_j a} \delta_{T_f T_{f_a}} \delta_{\pi\pi_a} + \delta_{k_k b} \delta_{j_j b} \delta_{T_f T_{f_a}} \delta_{\pi\pi_b}) \\
&- \frac{1}{2} \delta_{\Gamma\Gamma'} \delta_{\mu\mu'} \sum_{\lambda_i k_i \pi_i j_i Y_i T_i} \sum_L \frac{\sqrt{8(2L+1)}}{9} V_{\{\lambda_i \pi_i k_i j_i T_i\}}^L \\
&\times \left\{ (\delta_{\lambda_1, \frac{1}{2}} \delta_{\lambda_2, \frac{1}{2}} \delta_{\lambda_3, \frac{1}{2}} \delta_{\lambda_4, \frac{1}{2}}) (\delta_{\pi_1 \pi_a'} \delta_{\pi_b \pi_b'} \delta_{\pi_2 \pi_3} \delta_{\pi_4 \pi_a}) (\delta_{k_1 k_a'} \delta_{k_b k_b'} \delta_{k_2 k_3} \delta_{k_4 k_a}) (\delta_{j_1 j_a'} \delta_{j_b j_b'} \delta_{j_2 j_3} \delta_{j_4 j_a}) \right. \\
&\times (\delta_{T_1 T_a'} \delta_{T_b T_b'} \delta_{T_2 T_3} \delta_{T_4 T_a}) (\delta_{T_1 T_2} \delta_{T_3 T_4}) (\delta_{Y_1 Y_a'} \delta_{Y_b Y_b'} \delta_{Y_2 Y_3} \delta_{Y_4 Y_a}) (\delta_{Y_1 Y_2} \delta_{Y_3 T_4}) (-1)^{L-j_2+j_a} \frac{\delta_{j_a j_a'}}{2j_a+1} \\
&+ (\delta_{\lambda_1, \frac{1}{2}} \delta_{\lambda_2, \frac{1}{2}} \delta_{\lambda_3, -\frac{1}{2}} \delta_{\lambda_4, -\frac{1}{2}}) (\delta_{\pi_1 \pi_a'} \delta_{\pi_4 \pi_b'} \delta_{\pi_2 \pi_a} \delta_{\pi_3 \pi_b}) (\delta_{k_1 k_a'} \delta_{k_b k_b'} \delta_{k_2 k_a} \delta_{k_3 k_b}) (\delta_{j_1 j_a'} \delta_{j_4 j_b'} \delta_{j_2 j_a} \delta_{j_3 j_b}) \\
&\times (\delta_{T_1 T_a'} \delta_{T_4 T_b'} \delta_{T_2 T_a} \delta_{T_3 T_b}) (\delta_{T_1 T_2} \delta_{T_3 T_4}) (\delta_{Y_1 Y_a'} \delta_{Y_4 Y_b'} \delta_{Y_2 Y_a} \delta_{Y_3 Y_b}) (\delta_{Y_1 Y_2} \delta_{Y_3 T_4}) (-1)^{j_b-j_a+J} \begin{Bmatrix} j_b & j_a & J \\ j_a' & j_b' & L \end{Bmatrix} \\
&+ (\delta_{\lambda_1, -\frac{1}{2}} \delta_{\lambda_2, -\frac{1}{2}} \delta_{\lambda_3, \frac{1}{2}} \delta_{\lambda_4, \frac{1}{2}}) (\delta_{\pi_3 \pi_a'} \delta_{\pi_2 \pi_b'} \delta_{\pi_4 \pi_a} \delta_{\pi_1 \pi_b}) (\delta_{k_3 k_a'} \delta_{k_2 k_b'} \delta_{k_4 k_a} \delta_{k_1 k_b}) (\delta_{j_3 j_a'} \delta_{j_2 j_b'} \delta_{j_4 j_a} \delta_{j_1 j_b}) \\
&\times (\delta_{T_3 T_a'} \delta_{T_2 T_b'} \delta_{T_4 T_a} \delta_{T_1 T_b}) (\delta_{T_1 T_2} \delta_{T_3 T_4}) (\delta_{Y_3 Y_a'} \delta_{Y_2 Y_b'} \delta_{Y_4 Y_a} \delta_{Y_1 Y_b}) (\delta_{Y_1 Y_2} \delta_{Y_3 T_4}) (-1)^{j_b-j_a+J} \begin{Bmatrix} j_b & j_a & J \\ j_a' & j_b' & L \end{Bmatrix} \\
&+ (\delta_{\lambda_1, -\frac{1}{2}} \delta_{\lambda_2, -\frac{1}{2}} \delta_{\lambda_3, -\frac{1}{2}} \delta_{\lambda_4, -\frac{1}{2}}) (\delta_{\pi_a \pi_a'} \delta_{\pi_2 \pi_b'} \delta_{\pi_1 \pi_4} \delta_{\pi_3 \pi_b}) (\delta_{k_a k_a'} \delta_{k_2 k_b'} \delta_{k_1 k_4} \delta_{k_3 k_b}) (\delta_{j_a j_a'} \delta_{j_2 j_b'} \delta_{j_1 j_4} \delta_{j_3 j_b}) \\
&\times (\delta_{T_a T_a'} \delta_{T_2 T_b'} \delta_{T_1 T_4} \delta_{T_3 T_b}) (\delta_{T_1 T_2} \delta_{T_3 T_4}) (\delta_{Y_a Y_a'} \delta_{Y_2 Y_b'} \delta_{Y_1 Y_4} \delta_{Y_3 Y_b}) (\delta_{Y_1 Y_2} \delta_{Y_3 T_4}) (-1)^{L-j_1+j_b} \frac{\delta_{j_b j_b'}}{2j_b+1} \\
&+ (\delta_{\lambda_1, -\frac{1}{2}} \delta_{\lambda_2, \frac{1}{2}} \delta_{\lambda_3, \frac{1}{2}} \delta_{\lambda_4, -\frac{1}{2}}) (\delta_{\pi_3 \pi_a'} \delta_{\pi_b \pi_b'} \delta_{\pi_2 \pi_a} \delta_{\pi_1 \pi_4}) (\delta_{k_3 k_a'} \delta_{k_b k_b'} \delta_{k_2 k_a} \delta_{k_1 k_4}) (\delta_{j_3 j_a'} \delta_{j_b j_b'} \delta_{j_2 j_a} \delta_{j_1 j_4}) \\
&(\delta_{T_3 T_a'} \delta_{T_b T_b'} \delta_{T_2 T_a} \delta_{T_1 T_4}) (\delta_{T_1 T_2} \delta_{T_3 T_4}) (\delta_{Y_3 Y_a'} \delta_{Y_b Y_b'} \delta_{Y_2 Y_a} \delta_{Y_1 Y_4}) (\delta_{Y_1 Y_2} \delta_{Y_3 T_4}) (-1)^{L+j_1+j_a} \frac{\delta_{j_a j_a'}}{2j_a+1} \\
&+ (\delta_{\lambda_1, -\frac{1}{2}} \delta_{\lambda_2, \frac{1}{2}} \delta_{\lambda_3, \frac{1}{2}} \delta_{\lambda_4, -\frac{1}{2}}) (\delta_{\pi_a \pi_a'} \delta_{\pi_4 \pi_b'} \delta_{\pi_2 \pi_3} \delta_{\pi_1 \pi_b}) (\delta_{k_a k_a'} \delta_{k_4 k_b'} \delta_{k_2 k_3} \delta_{k_1 k_b}) (\delta_{j_a j_a'} \delta_{j_4 j_b'} \delta_{j_2 j_3} \delta_{j_1 j_b}) \\
&(\delta_{T_a T_a'} \delta_{T_4 T_b'} \delta_{T_2 T_3} \delta_{T_1 T_b}) (\delta_{T_1 T_2} \delta_{T_3 T_4}) (\delta_{Y_a Y_a'} \delta_{Y_4 Y_b'} \delta_{Y_2 Y_3} \delta_{Y_1 Y_b}) (\delta_{Y_1 Y_2} \delta_{Y_3 T_4}) (-1)^{L+j_2+j_b} \frac{\delta_{j_b j_b'}}{2j_b+1} \left. \right\}. \tag{D1}
\end{aligned}$$

The backward matrix elements are

$$\begin{aligned}
& B_{a'b';\Gamma'; a,b;\Gamma} = -\frac{1}{2} \delta_{\Gamma\Gamma'} \delta_{\mu\mu'} \sum_{\lambda_i k_i \pi_i j_i Y_i T_i} \sum_L \frac{\sqrt{8(2L+1)}}{9} V_{\{\lambda_i \pi_i k_i j_i T_i\}}^L \\
&\times \left\{ (\delta_{\lambda_1, \frac{1}{2}} \delta_{\lambda_2, -\frac{1}{2}} \delta_{\lambda_3, \frac{1}{2}} \delta_{\lambda_4, -\frac{1}{2}}) (\delta_{\pi_3 \pi_a'} \delta_{\pi_2 \pi_b'} \delta_{\pi_1 \pi_a} \delta_{\pi_4 \pi_b}) (\delta_{k_3 k_a'} \delta_{k_2 k_b'} \delta_{k_1 k_a} \delta_{k_4 k_b}) (\delta_{j_3 j_a'} \delta_{j_2 j_b'} \delta_{j_1 j_a} \delta_{j_4 j_b}) \right. \\
&\times (\delta_{T_3 T_a'} \delta_{T_2 T_b'} \delta_{T_1 T_a} \delta_{T_4 T_b}) (\delta_{T_1 T_2} \delta_{T_3 T_4}) (\delta_{Y_3 Y_a'} \delta_{Y_2 Y_b'} \delta_{Y_1 Y_a} \delta_{Y_4 Y_b}) (\delta_{Y_1 Y_2} \delta_{Y_3 T_4}) \begin{Bmatrix} j_b' & j_a' & J \\ j_b & j_a & L \end{Bmatrix} \\
&+ (\delta_{\lambda_1, \frac{1}{2}} \delta_{\lambda_2, -\frac{1}{2}} \delta_{\lambda_3, \frac{1}{2}} \delta_{\lambda_4, -\frac{1}{2}}) (\delta_{\pi_1 \pi_a'} \delta_{\pi_4 \pi_b'} \delta_{\pi_3 \pi_a} \delta_{\pi_2 \pi_b}) (\delta_{k_1 k_a'} \delta_{k_4 k_b'} \delta_{k_3 k_a} \delta_{k_2 k_b}) (\delta_{j_1 j_a'} \delta_{j_4 j_b'} \delta_{j_3 j_a} \delta_{j_2 j_b}) \\
&\times (\delta_{T_1 T_a'} \delta_{T_4 T_b'} \delta_{T_3 T_a} \delta_{T_2 T_b}) (\delta_{T_1 T_2} \delta_{T_3 T_4}) (\delta_{Y_1 Y_a'} \delta_{Y_4 Y_b'} \delta_{Y_3 Y_a} \delta_{Y_2 Y_b}) (\delta_{Y_1 Y_2} \delta_{Y_3 T_4}) \begin{Bmatrix} j_b' & j_a' & J \\ j_b & j_a & L \end{Bmatrix} \left. \right\}. \tag{D2}
\end{aligned}$$

### Appendix E: Renormalization procedure.

In this appendix we elaborate on the renormalization of the quark masses  $m_{u,d}$ ,  $m_s$  and the interaction parameters  $\alpha$  and  $\beta$ , *at least approximately*, when the cut-off, given by the maximal number of oscillation quanta  $N_{\text{cut}} \geq N_0$ , is changed. We have selected a low-energy renormalization point denoted by  $N_0 = 3$ , therefore in this renormalization procedure  $N_{\text{cut}}$  always increases.

After the diagonalization of the kinetic term (Eqs. (6) and (7)), the Hamiltonian has the following structure

$$\mathbf{H} = \sum_p \varepsilon_p \mathbf{n}_p - \alpha \frac{1}{\mathbf{r}} + \beta \mathbf{r} \quad , \quad (\text{E1})$$

where  $\mathbf{r}$  is a short-hand notation for the linear interaction,  $\frac{1}{\mathbf{r}}$  for the standard Coulomb interaction and  $\varepsilon_p$  is the single-particle energy in the state  $p$ . The operator  $\mathbf{n}_p$  is a short-hand notation for the sum of the quark and antiquark number operators related to the state  $p$ .

The meson states we construct (approximately) fulfill the Schrödinger equation  $\mathbf{H} | \Psi_i \rangle = E_i | \Psi_i \rangle$ . We multiply the equation from the left with  $\langle \Psi_i |$ , using the notation  $\langle \dots \rangle$  for  $\langle \Psi_i | \dots | \Psi_i \rangle$ , to arrive at

$$\langle \mathbf{H} \rangle_{N_{\text{cut}}} = \sum_p \varepsilon_p^{N_{\text{cut}}} \langle \mathbf{n}_p \rangle_{N_{\text{cut}}} - \alpha_{N_{\text{cut}}} \left\langle \frac{1}{\mathbf{r}} \right\rangle_{N_{\text{cut}}} + \beta_{N_{\text{cut}}} \langle \mathbf{r} \rangle_{N_{\text{cut}}} \quad , \quad (\text{E2})$$

where we have explicitly indicated the dependence of the expectation values on the cutoff  $N_{\text{cut}}$ . The first contribution on the R.H.S. is the prediagonalized kinetic energy. Its eigenstates correspond to states of free motion and, if no boundary condition is imposed, the eigenvalues have to be continuous. In this case the harmonic oscillator basis is not good at all. However, we consider *confined* particles, and fixing the energy of the first single-particle state  $\varepsilon_1$  to a definite value independent of  $N_{\text{cut}}$  (see Table VI) amounts to defining a scale or extension for the system, which is proportional to the harmonic oscillator length  $\frac{1}{\sqrt{B_0}}$ .

Now assume that, for a given value of the cut-off  $N_0$ , the parameters of the Hamiltonian are adjusted to reproduce some low lying state (*e.g.*, the pion state). The expectation value of the Hamiltonian is then

$$\langle \mathbf{H} \rangle_{N_0} = \sum_p \varepsilon_p^{N_0} \langle \mathbf{n}_p \rangle_{N_0} - \alpha_{N_0} \left\langle \frac{1}{\mathbf{r}} \right\rangle_{N_0} + \beta_{N_0} \langle \mathbf{r} \rangle_{N_0} \quad . \quad (\text{E3})$$

Its relation to (E2) with a finite cut-off at  $N_{\text{cut}}$  is

$$\langle \mathbf{H} \rangle_{N_{\text{cut}}} = \langle \mathbf{H} \rangle_{N_0} + \langle \mathbf{H} \rangle_{N_{\text{cut}} > N_0} \quad (\text{E4})$$

where the last term refers to the contributions for  $N_{\text{cut}} > N_0$ . Equation (E4) can be extended to any kind of operator, replacing in the equations above the Hamiltonian  $\mathbf{H}$  with the operator  $\mathbf{O}$ , which can be  $\mathbf{r}$  or any of those appearing in (E1).

The *renormalization condition* is that the (low-lying) energies, as the observables, do not change when the cut-off is increased (or decreased). In order to achieve this, we first discuss the renormalization of the masses and then the renormalization of the interaction parameters  $\alpha$  and  $\beta$ .

The mass parameters are contained implicitly in the single-particle energies  $\varepsilon_p^{N_0}$ . One contribution to  $\varepsilon_p^{N_0}$  comes from the kinetic energy, which is not subject to renormalization, and the other from the masses of the different types of quarks, which have to be renormalized. The renormalization of the quark masses can be achieved by a multiplicative factor, *i.e.*,

$$m_{N_{\text{cut}}}^f \approx m_{N_0}^f \sqrt{x_{N_{\text{cut}}}^f} \quad , \quad (\text{E5})$$

where we have taken into account that the factor may depend on the flavor of the quark,  $q = u, d$  or  $s$ .

The purpose of Eq. (E5) is to guarantee that the effective single-particle energies ( $m_q^{eff} = \varepsilon_{1, \frac{1}{2}, \pm \frac{1}{2}, \frac{1}{2}}$  and  $m_s^{eff} = \varepsilon_{1, \frac{1}{2}, 0, 0}$ ) remain unchanged as functions of  $N_{\text{cut}}$ , see Table VI. Therefore, the renormalization of the interaction can be performed independently.

We shall now describe the renormalization of the interaction:

Let us take as an example the linear interaction operator; then (E4), multiplied by the interaction parameter, can be rewritten as

$$\begin{aligned} \beta_{N_{\text{cut}}} \langle \mathbf{r} \rangle_{N_{\text{cut}}} &= \beta_{N_{\text{cut}}} \left( 1 + \frac{\langle \mathbf{r} \rangle_{N_{\text{cut}} > N_0}}{\langle \mathbf{r} \rangle_{N_0}} \right) \langle \mathbf{r} \rangle_{N_0} \\ &= \beta_{N_0} \langle \mathbf{r} \rangle_{N_0} \quad , \end{aligned} \quad (\text{E6})$$

hence the relation between  $\beta_{N_0}$  and the  $\beta_{N_{\text{cut}}}$  is

$$\begin{aligned}\beta_{N_{\text{cut}}} &= \beta_{N_0} / \sqrt{x_{N_{\text{cut}}}} \\ \sqrt{x_{N_{\text{cut}}}} &= \left( 1 + \frac{\langle \mathbf{r} \rangle_{N_{\text{cut}} > N_0}}{\langle \mathbf{r} \rangle_{N_0}} \right) .\end{aligned}\quad (\text{E7})$$

This guarantees the same expectation value via the renormalization of  $\beta$  as a function of the cut-off. Equation (E7) incorporates the contributions from  $N$  larger than  $N_0$ . The square root is introduced for convenience. An analogous argument applies to the  $\frac{1}{r}$  interaction, and assuming that the relation  $\langle \frac{1}{r} \rangle \approx \frac{1}{\langle r \rangle}$  is fulfilled, we have  $\alpha_{N_{\text{cut}}} \approx \alpha_{N_0} \sqrt{x_{N_{\text{cut}}}}$ .

We have performed numerical diagonalizations, increasing  $N$  from 3 to 13 in steps of 2 and determining  $x_{N_{\text{cut}}}$  and  $x_{N_{\text{cut}}}^f$  such that the first single-particle energy remains approximately constant, see Table VI. Changing the masses and interaction constants according to the above equations results in an approximately invariant RPA spectrum. Even though we cannot determine exact expressions for the renormalization functions because of the highly non-linear structure of the equations, a rough estimate of the factors  $x_{N_{\text{cut}}}$  and  $x_{N_{\text{cut}}}^f$  is given by

$$\begin{aligned}x_{N_{\text{cut}}} &\approx 1 + t_1 (N_{\text{cut}} - N_0)^{t_2} \\ x_{N_{\text{cut}}}^f &\approx 1 + t_1^f (N_{\text{cut}} - N_0)^{t_2^f} ,\end{aligned}\quad (\text{E8})$$

where  $t_1, t_2, t_1^f, t_2^f$  are constants listed in Table VII, and  $x_{N_{\text{cut}}}$  and  $x_{N_{\text{cut}}}^f$  have to satisfy the boundary conditions  $x_{N_0} = 1$  and  $x_{N_0}^f = 1$ , respectively.

- 
- [1] W. Bietenholz, *Int. J. Mod. Phys. E* **25**, 1642008 (2016).
  - [2] Z. Fodor and C. Hoelbling, *Rev. Mod. Phys.* **84**, 449 (2012).
  - [3] S. Aoki *et al.* (FLAG Working Group), *Eur. Phys. J. C* **74**, 2890 (2014).
  - [4] J. J. Dudek *et al.*, *Phys. Rev. D* **83**, 111502(R) (2011).
  - [5] A. Bashir *et al.*, *Comm. Theor. Phys.* **58**, 79 (2012).
  - [6] P. O. Hess, S. A. Lerma H., J. C. López V., C. R. Stephens and A. Weber, *Eur. Phys. J. C* **9**, 121 (1999).
  - [7] S. Lerma H., S. Jesgarz, P. O. Hess, O. Civitarese and M. Reboiro, *Phys. Rev. C* **67**, 055209 (2003).
  - [8] M. V. Nuñez, S. H. Lerma, P. O. Hess, S. Jesgarz, O. Civitarese and M. Reboiro, *Phys. Rev. C* **70**, 035208 (2004).
  - [9] N. H. Christ and T. D. Lee, *Phys. Rev. D* **22**, 939 (1980).
  - [10] T. D. Lee, *Particle Physics and Introduction to Field Theory* (Harwood Academic Publishers, New York, 1981).
  - [11] G. S. Bali *et al.* (UKQCD Collaboration), *Phys. Lett. B* **309**, 378 (1993).
  - [12] C. J. Morningstar and M. Peardon, *Phys. Rev. D* **60**, 034509 (1999).
  - [13] A. Szczepaniak, E. S. Swanson, C. R. Ji and S. R. Cotanch, *Phys. Rev. Lett.* **76**, 2011 (1996).
  - [14] A. P. Szczepaniak and E. S. Swanson, *Phys. Lett. B* **577**, 61 (2003).
  - [15] P. Guo, A. P. Szczepaniak, G. Galata, A. Vassallo and E. Santopinto, *Phys. Rev. D* **78**, 056003 (2008).
  - [16] P. Guo, T. Yépez-Martínez and A. P. Szczepaniak, *Phys. Rev. D* **89**, 116005 (2014).
  - [17] J. J. Dudek, R. G. Edwards and D. G. Richards, *Phys. Rev. D* **73**, 074507 (2006).
  - [18] J. J. Dudek, R. G. Edwards and C. E. Thomas, *Phys. Rev. D* **79**, 094504 (2009).
  - [19] H. Reinhardt, D. R. Campagnari and A. P. Szczepaniak, *Phys. Rev. D* **84**, 045006 (2011).
  - [20] T. Yépez-Martínez, A. P. Szczepaniak and H. Reinhardt, *Phys. Rev. D* **86**, 076010 (2012).
  - [21] J. Engels, F. Karsch, H. Satz and I. Montvay, *Nucl. Phys. B* **205**, 545 (1982).
  - [22] G. Boyd *et al.*, *Nucl. Phys. B* **469**, 419 (1996).
  - [23] A. P. Szczepaniak and E. Swanson, *Phys. Rev. D* **65**, 025012 (2001).
  - [24] P. O. Hess and A. P. Szczepaniak, *Phys. Rev. C* **73**, 025201 (2006).
  - [25] T. Yépez-Martínez, P. O. Hess, A. P. Szczepaniak and O. Civitarese, *Phys. Rev. C* **81**, 045204 (2010).
  - [26] T. Yépez-Martínez, O. Civitarese and P. O. Hess, *Int. J. Mod. Phys. E* **25**, 1650067 (2016).
  - [27] T. Yépez-Martínez, O. Civitarese and P. O. Hess, *Int. J. Mod. Phys. E* **26**, 1750012 (2017).
  - [28] C. Feuchter and H. Reinhardt, *Phys. Rev. D* **70**, 105021 (2004).
  - [29] F. J. Llanes-Estrada and S. R. Cotanch, *Nucl. Phys. A* **697**, 303 (2002).
  - [30] F. J. Llanes-Estrada and S. R. Cotanch, *Phys. Rev. Lett.* **84**, 1102 (2000).
  - [31] J. Escher and J. P. Draayer, *J. Math. Phys.* **39**, 5123 (1998).
  - [32] P. Ring and P. Schuck, *The Nuclear Many Body Problem* (Springer, Heidelberg, 1980).
  - [33] Particle Data Group (C. Patrignani *et al.*), *Chin. Phys. C* **40**, 100001 (2016).
  - [34] A. De Rújula, H. Georgi and S. L. Glashow, *Phys. Rev. D* **12**, 147 (1975).
  - [35] J. J. Dudek, *Phys. Rev. D* **84**, 074023 (2011).

- [36] F.-G. Cao, Phys. Rev. D **85**, 057501 (2012).
- [37] A. Bramon, R. Escribano and M. Scadron, Eur. Phys. J. C **7**, 271 (1999).
- [38] S. Stone and L. Zhang, Phys. Rev. Lett. **111**, 062001 (2013).
- [39] G. Eichmann, C. S. Fischer and W. Heupel, Phys. Lett. B **753**, 282 (2016).
- [40] J. A. Oller, Nucl. Phys. A **727**, 353 (2003).
- [41] O. Civitarese, P. O. Hess and D. A. Amor-Quiroz, Int. J. Mod. Phys. E **22**, 135071 (2013).
- [42] M. Moshinsky, Nucl. Phys. **13**, 104 (1959).
- [43] G. P. Kamuntavicius, R. K. Kalinauskas, B. R. Barrett, S. Mickeviciu and D. Germanas, Nucl. Phys. A **695**, 191 (2001).
- [44] D. A. Varshalovich, A. N. Moskalev and V. K. Khersonskii, *Quantum Theory of Angular Momentum* (World Scientific, 1988)